

EJC2017

New views on radioactivity

Les Issambres, France

24-29/09/2017

DATING METHODS IN PREHISTORY DURING QUATERNARY PERIOD

Christophe Falguères

UMR7194 "Histoire naturelle de l'Homme préhistorique"

Muséum national d'histoire naturelle

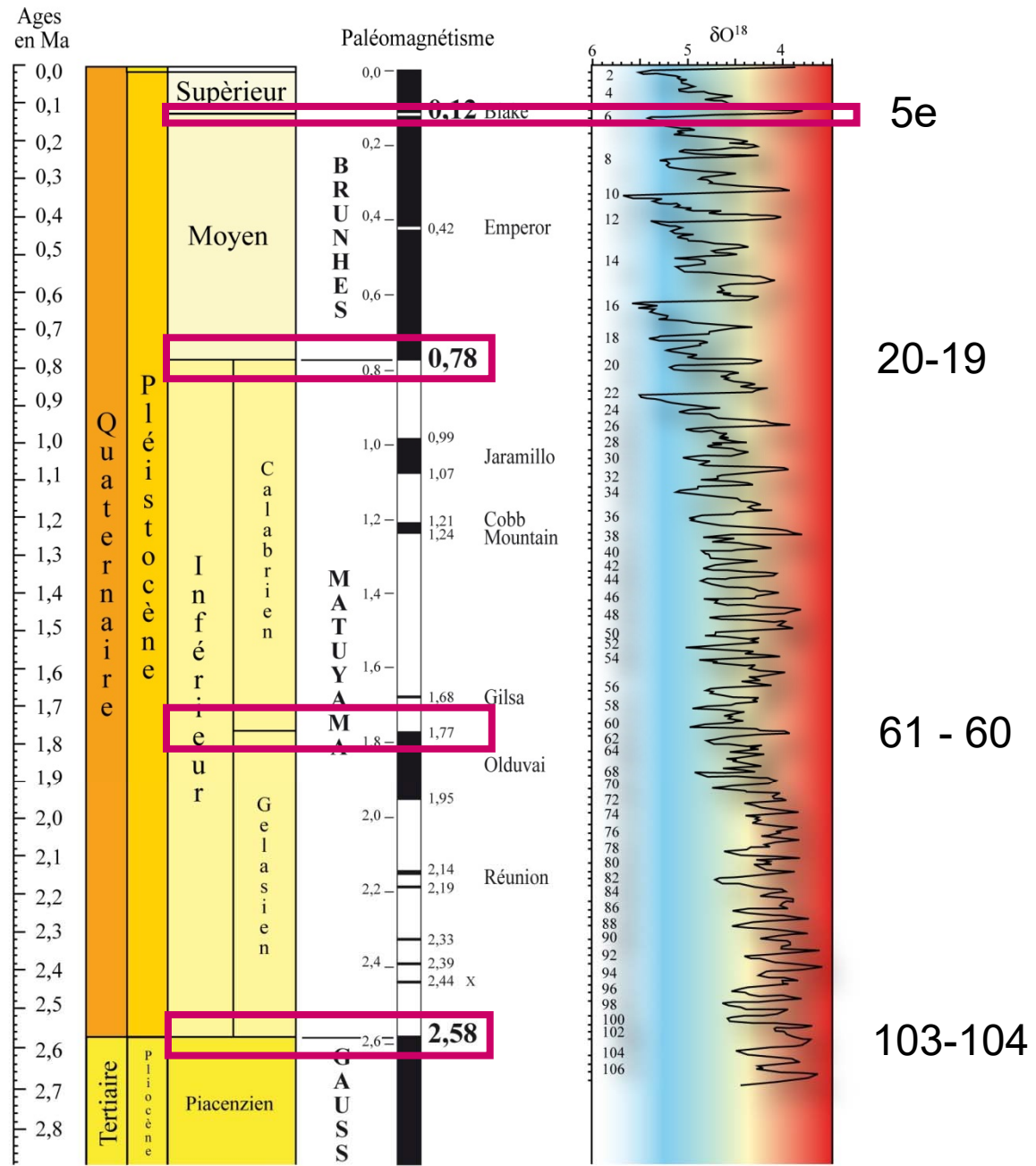
Institut de Paléontologie Humaine,

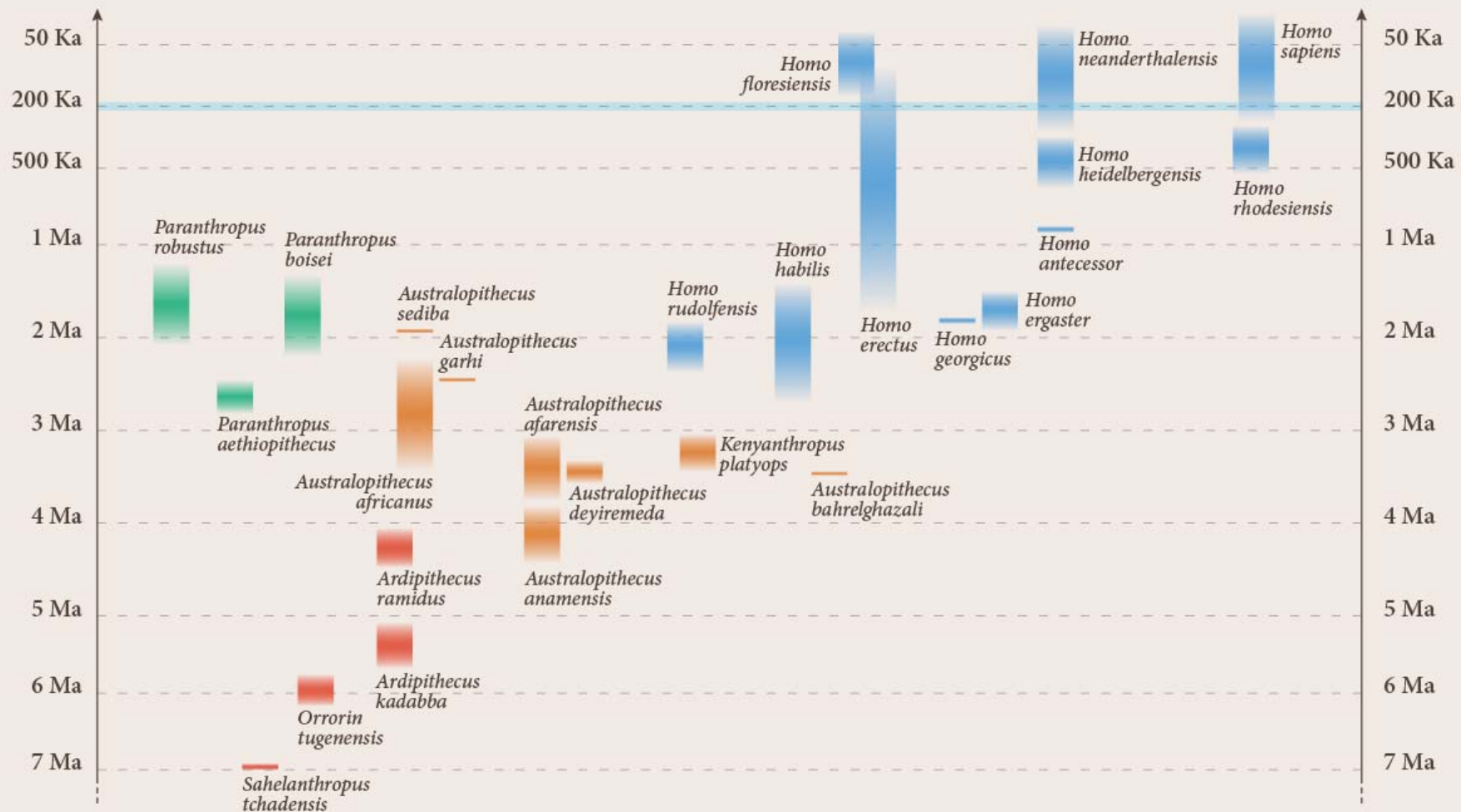
1, rue René Panhard,

75013, Paris, France

christophe.falgueres@mnhn.fr







Principales méthodes utilisées en Géochronologie

Méthodes « Naturalistes »

- Stratigraphie
- Biostratigraphie
- Varves
- Dendrochronologie
- Téphrochronologie
- Paléomagnétisme
- Isotopes de l'oxygène

Méthodes fondées sur un phénomène chimique

- Racémisation des acides aminés
- Hydratation de l'obsidienne

Méthodes fondées sur la croissance ou la décroissance radioactive

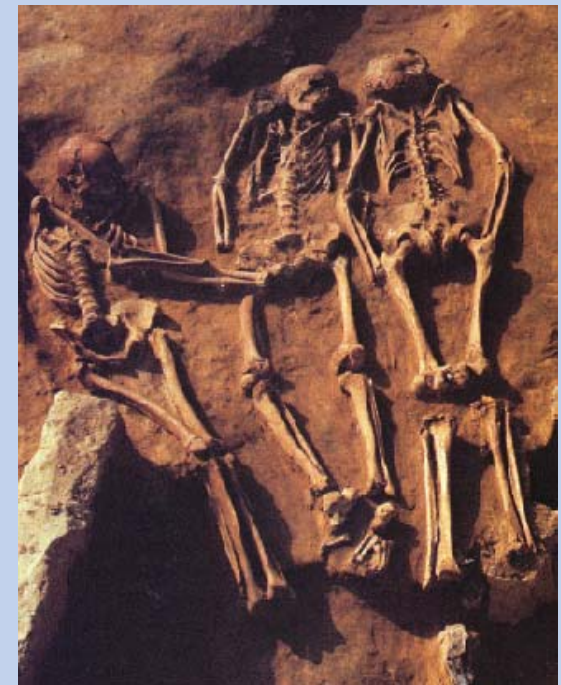
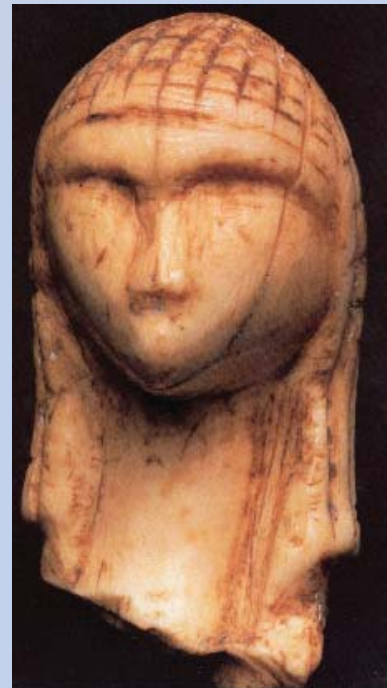
- Radiocarbone, ^{14}C
- Famille de l'Argon, Ar/Ar, K/Ar
- Séries de l'uranium, Th/U, Pa/U
- Autres cosmonucléides, Al/Be

Méthodes fondées sur les dommages créés dans les minéraux par la radioactivité naturelle

- Trace de fission
- Résonance de Spin Électronique, ESR
- Luminescence, TL, OSL, TT-OSL, IRSL



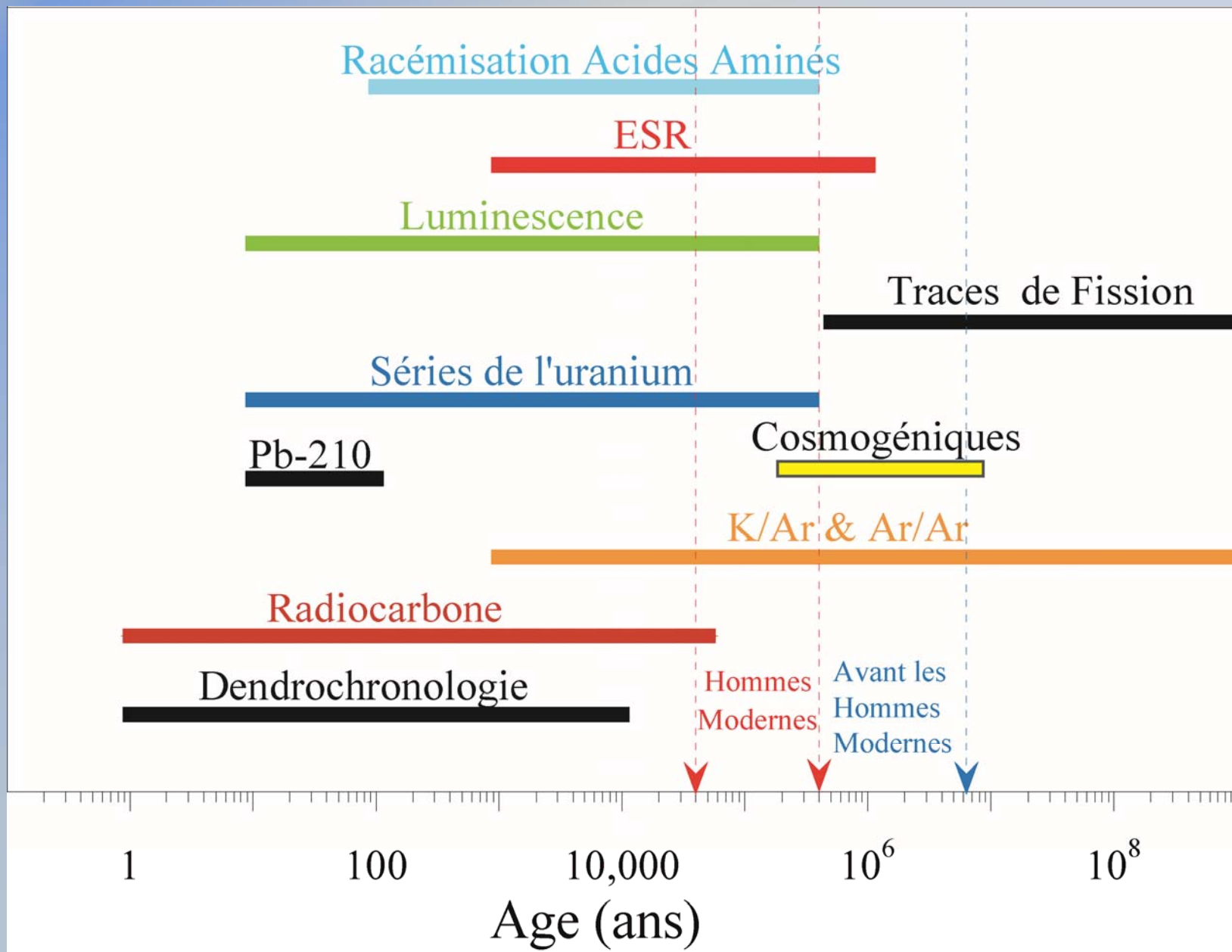
What we want to date... ..





... and what we really date...





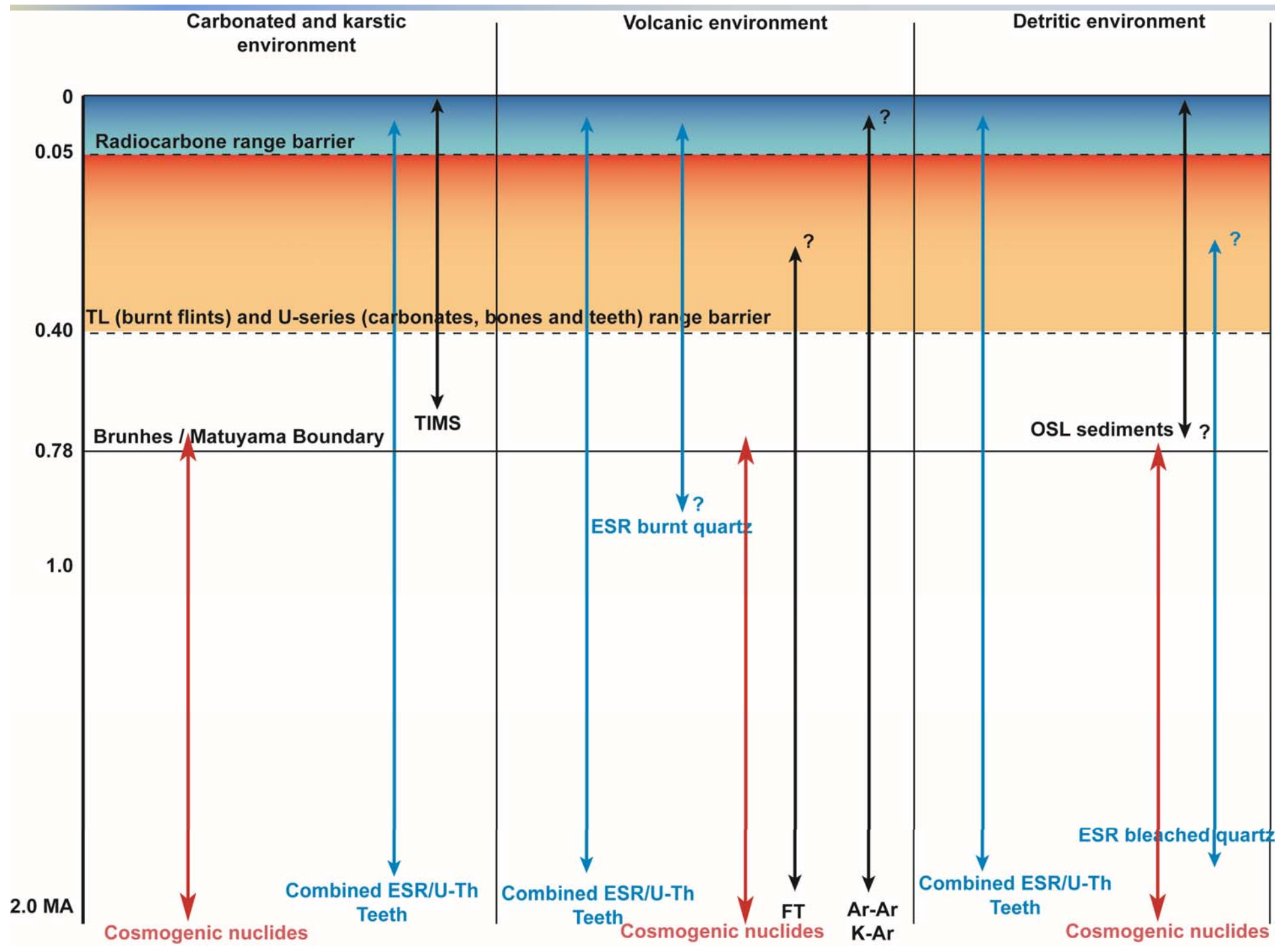
Problems related to the dating methods

Range of applicability

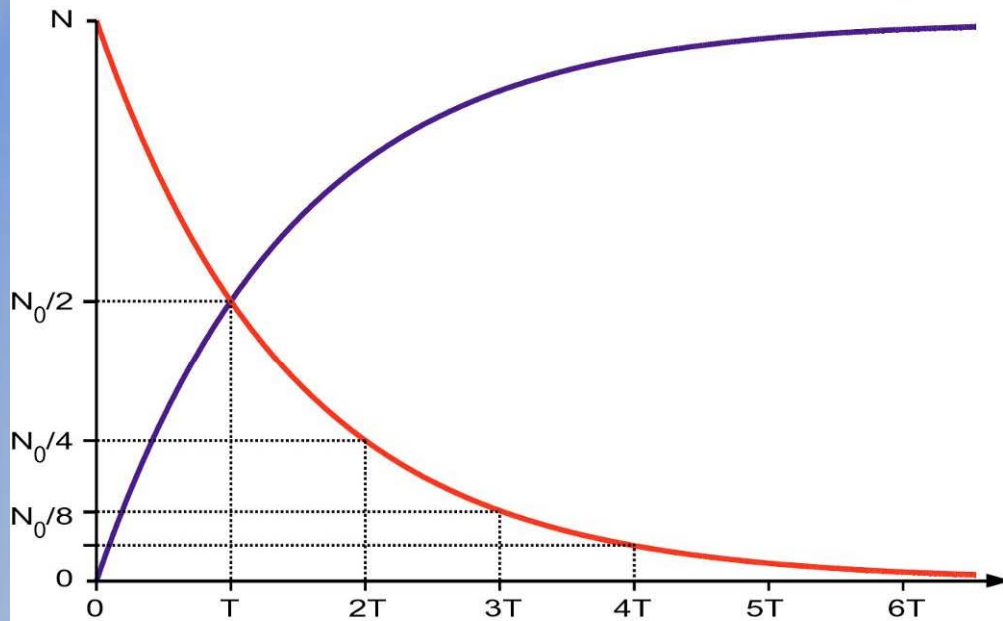
Uranium uptake => closed system or opened system

Suitability of the samples

Stratigraphic control and heterogeneity of the layers



Isotopic dating methods



$$N(t) = N_0 (1 - e^{-0.693t/T})$$

Élément fils

$$N(t) = N_0 e^{-\lambda t}$$

$$N(t) = N_0 e^{-0.693t/T}$$

Élément père

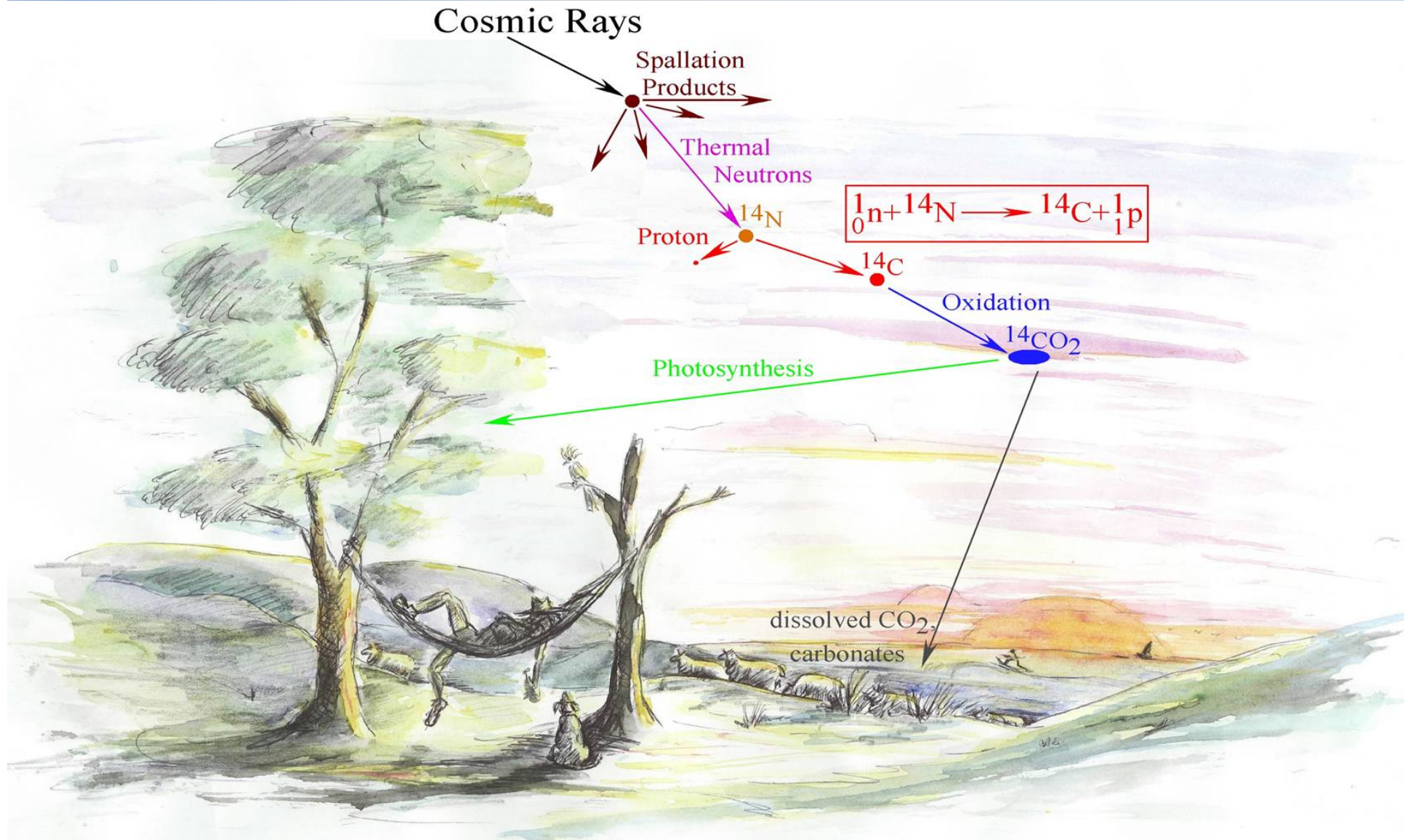
Half-life

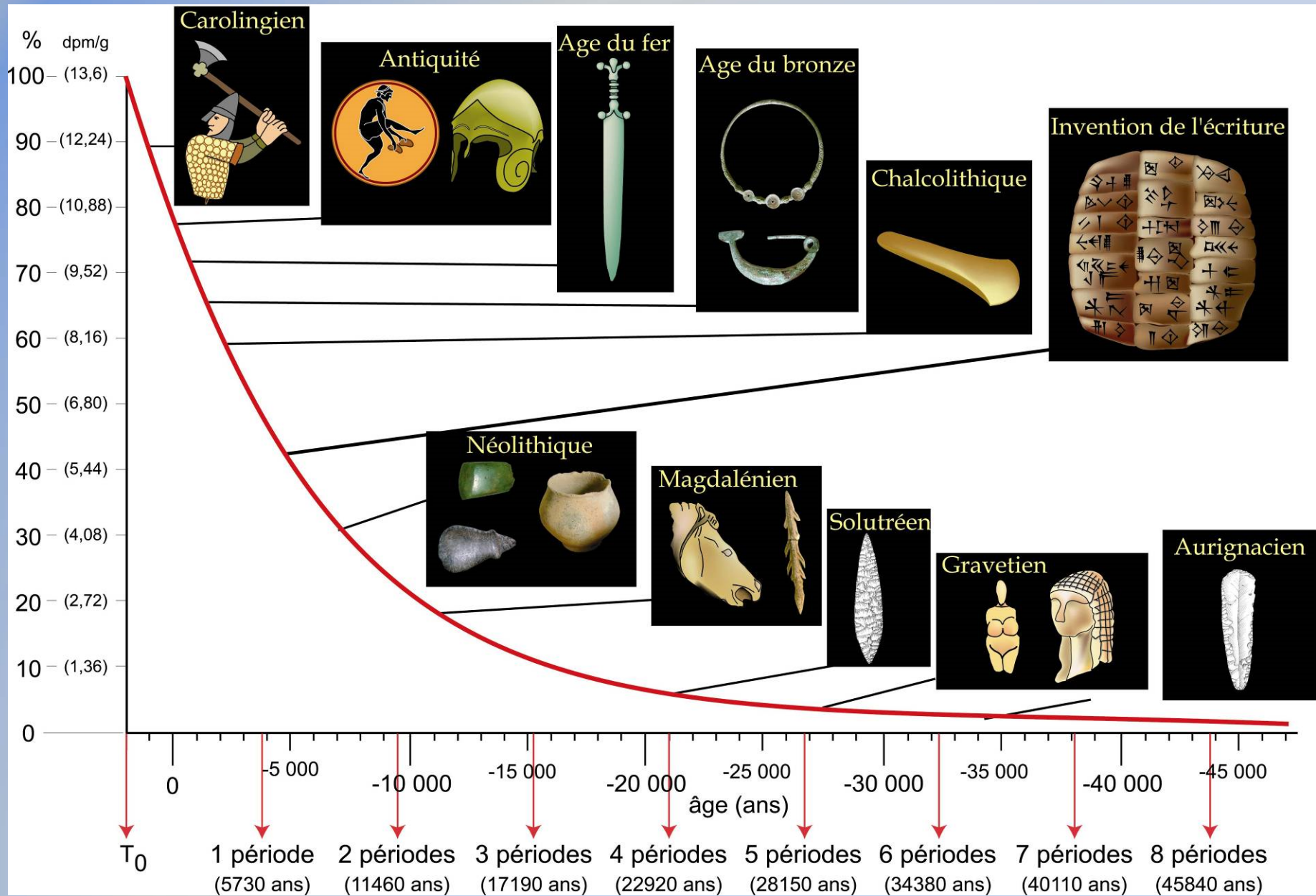
^{14}C : 5,730 ka

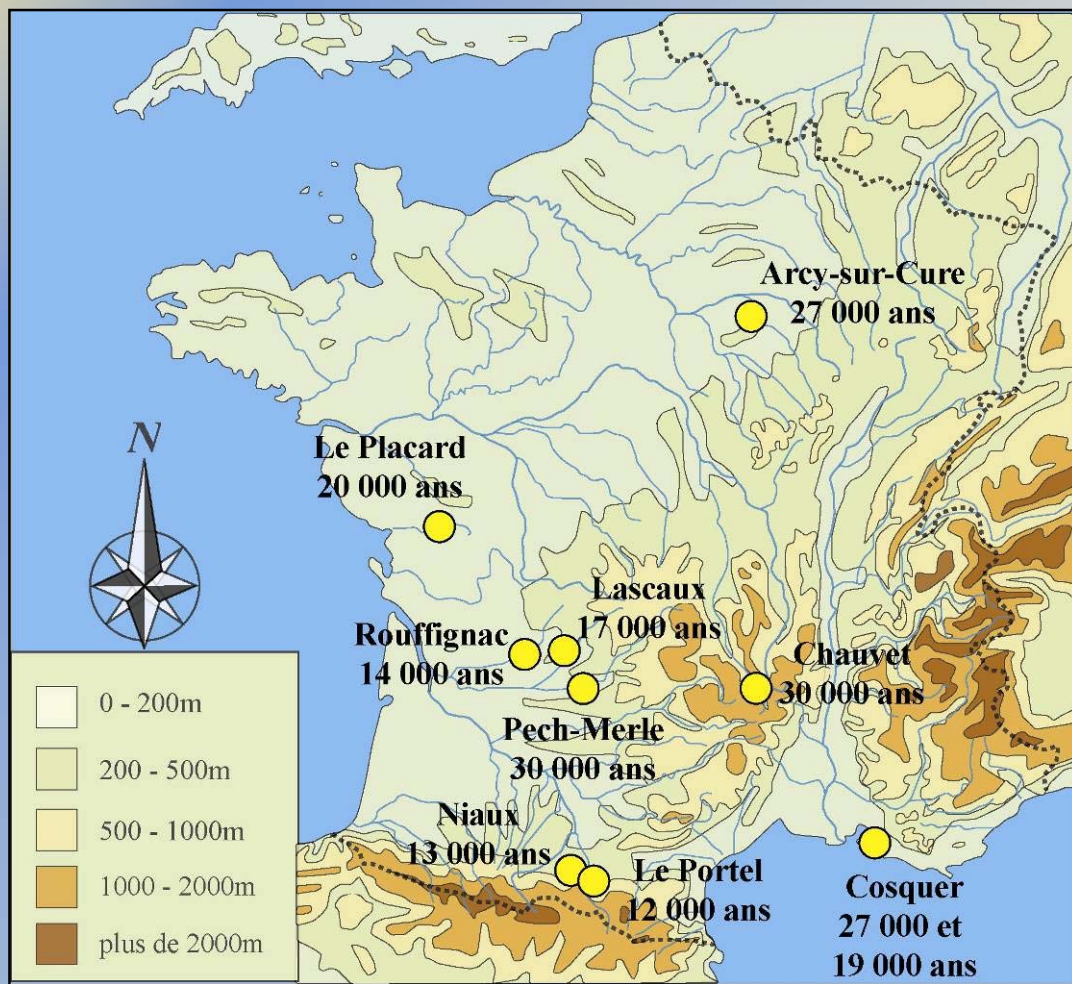
^{230}Th : 75,200 ka

^{40}K : 1 250 Ma

Radiocarbon method







Arcy-sur-Cure



Chauvet



Lascaux



Niaux



Le Portel



Cosquer

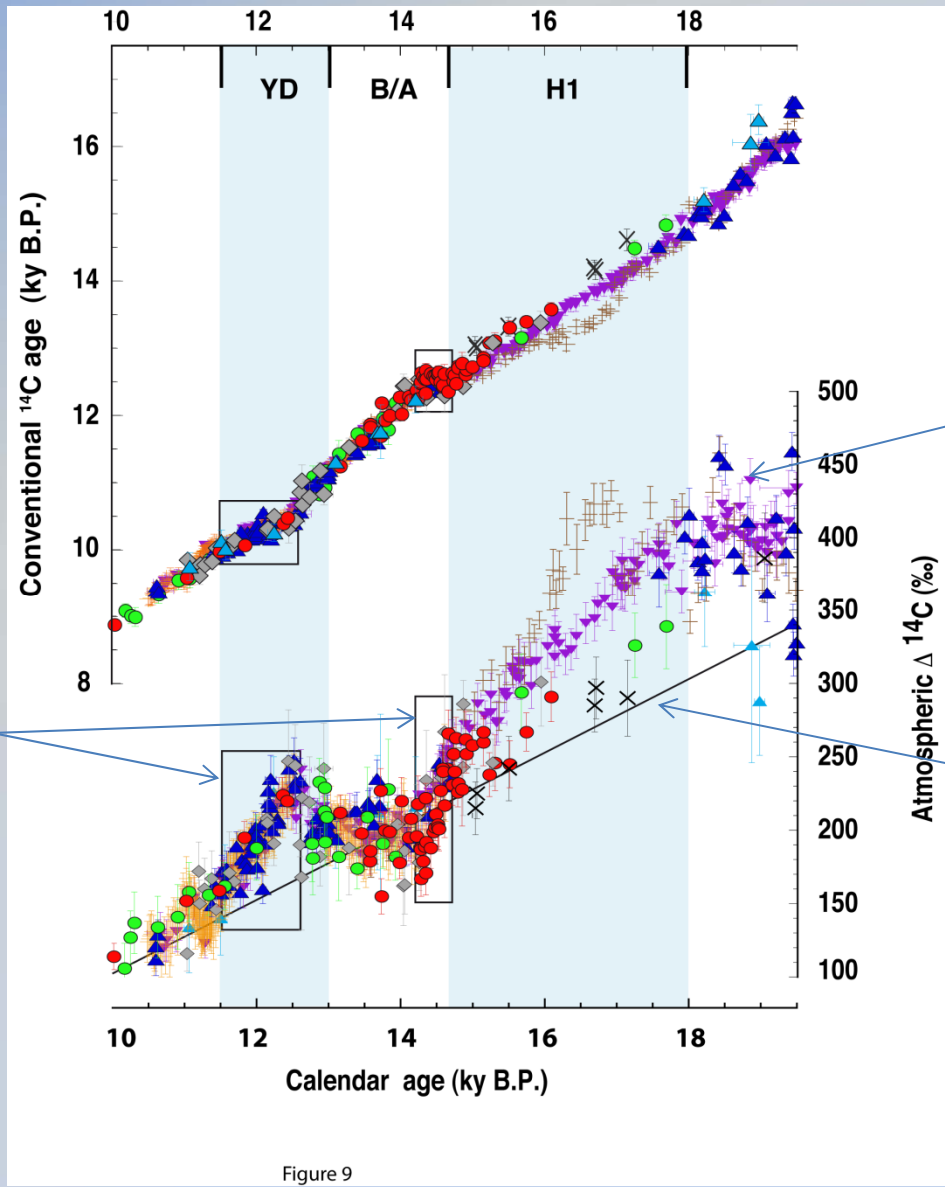


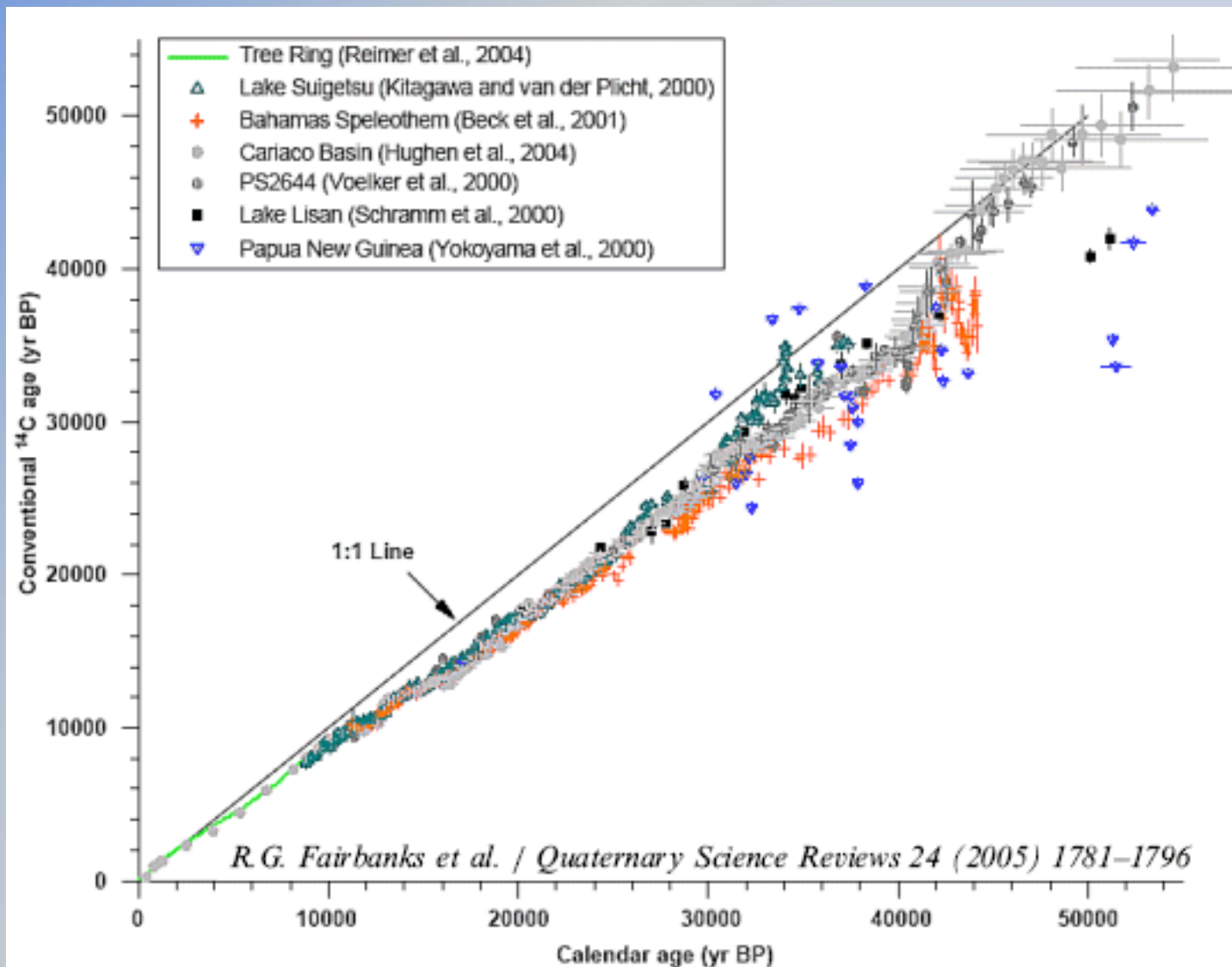
Figure 9

Rapid drops in the atmospheric ^{14}C record corresponding to ^{14}C age plateaus

Speleothem, Hulu Cave, China

Long-term trend of atmospheric ^{14}C

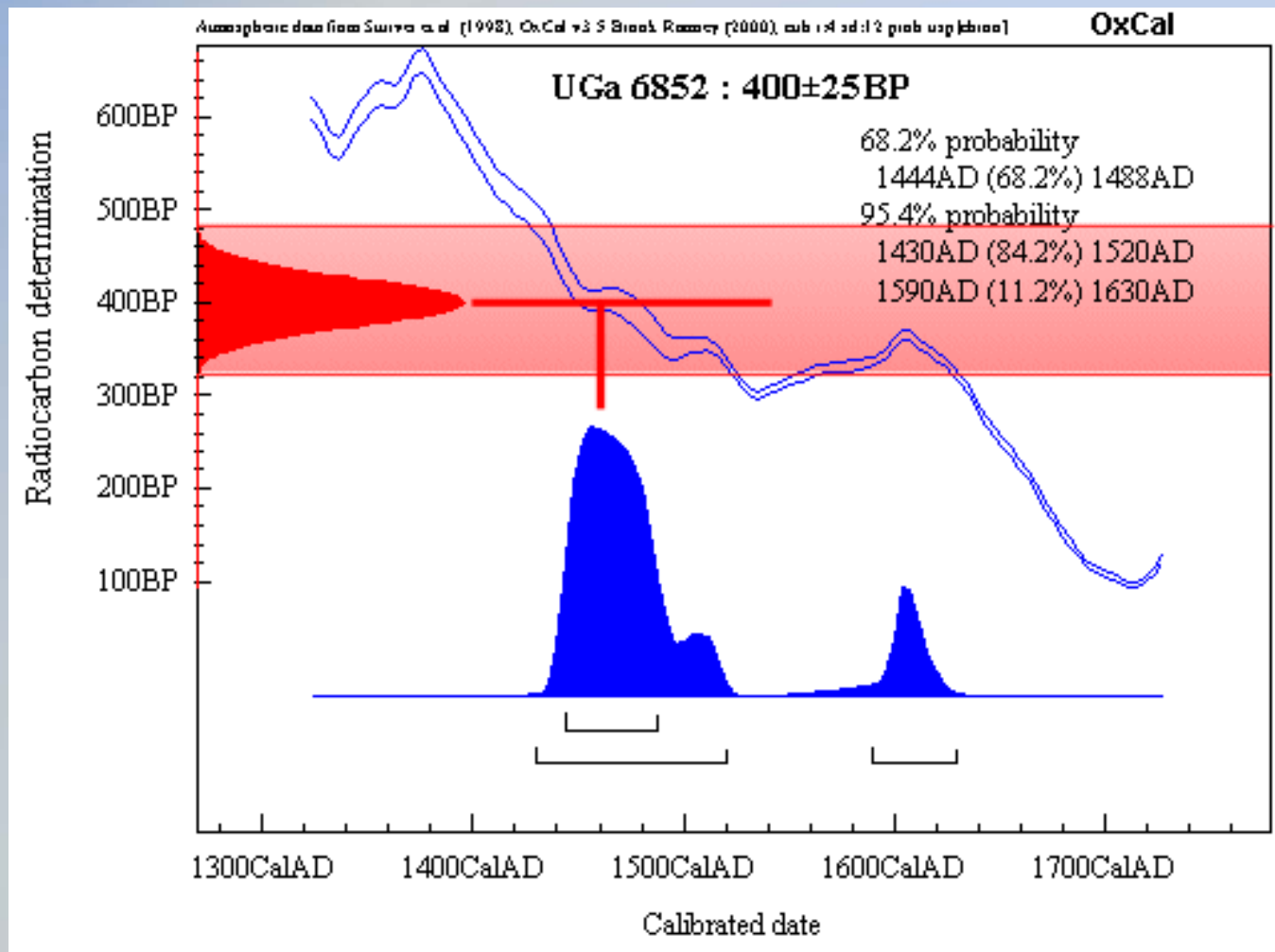
Extremely large variations of atmospheric ^{14}C concentration during the whole deglaciation period implying a correction of the ages (Durand et al., Radiocarbon, 2013)



^{14}C ages can be presented as ^{14}C BP (conventional age) based on the proportion of radiocarbon in the sample without any variation of the atmospheric radiocarbon concentration.

They can be calibrated (INTCAL13 using data sets from ^{14}C measurements on tree rings, plant macrofossils, speleothems, corals, foraminifera; **Reimer et al., Radiocarbon, 2013**)

^{14}C cal. BP or directly in calendar ages BP, BC or AD



CHAUVET CAVE

Distribution of ^{14}C dated Samples

Cave floor charcoal - Parietal Marks - Animal Bones

KEY

Distribution of ^{14}C dated samples

Charcoals

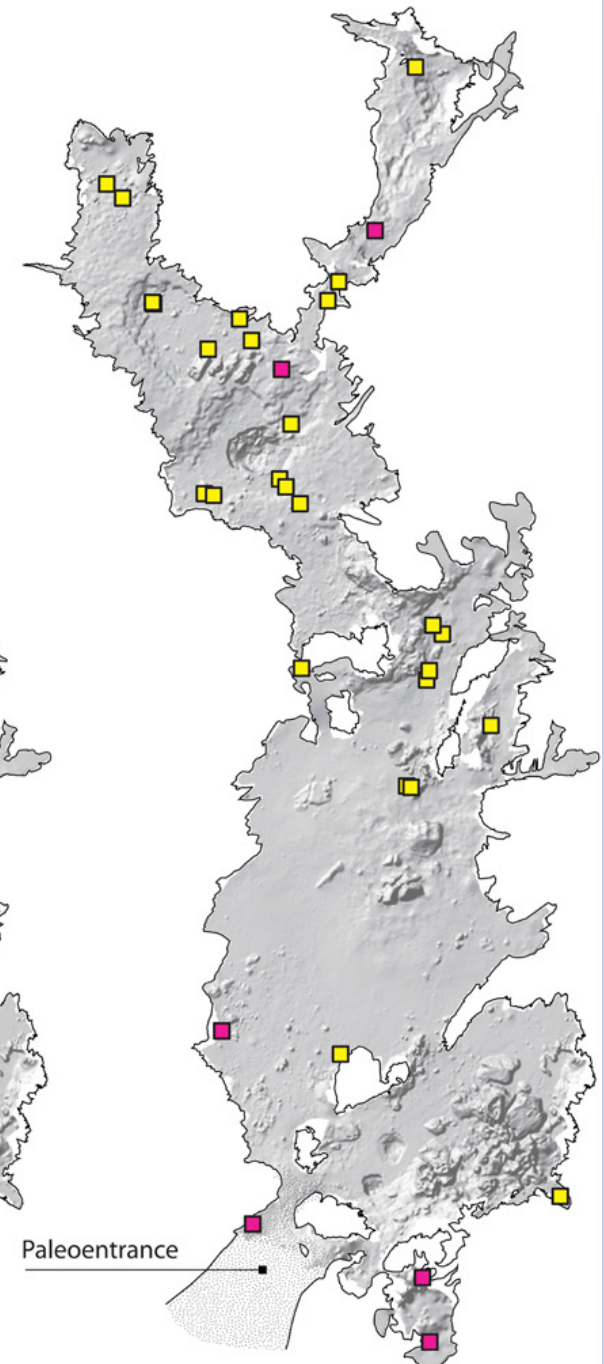
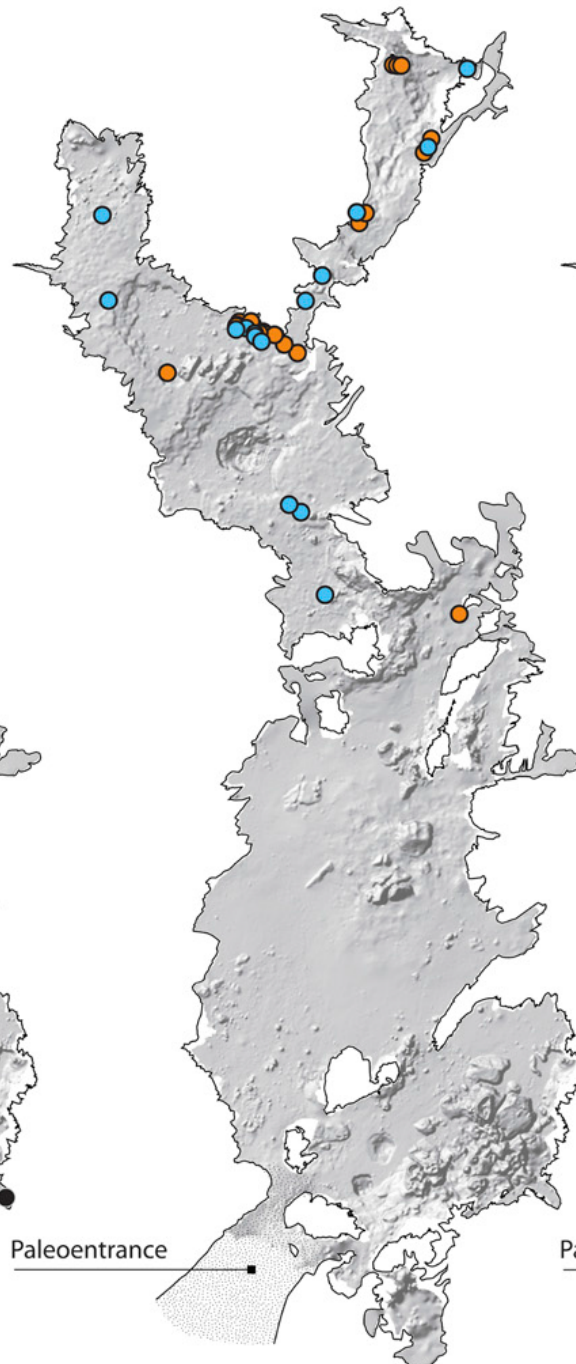
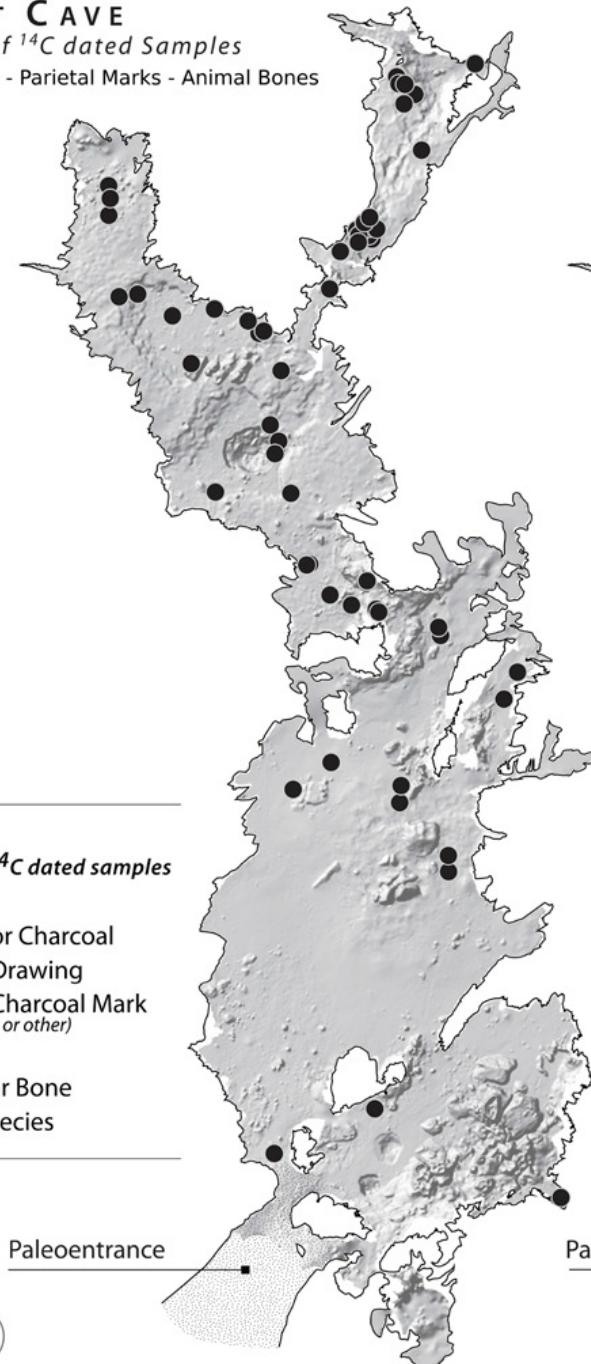
- Cave floor Charcoal
- Parietal Drawing
- Parietal Charcoal Mark
(Torch Mark or other)

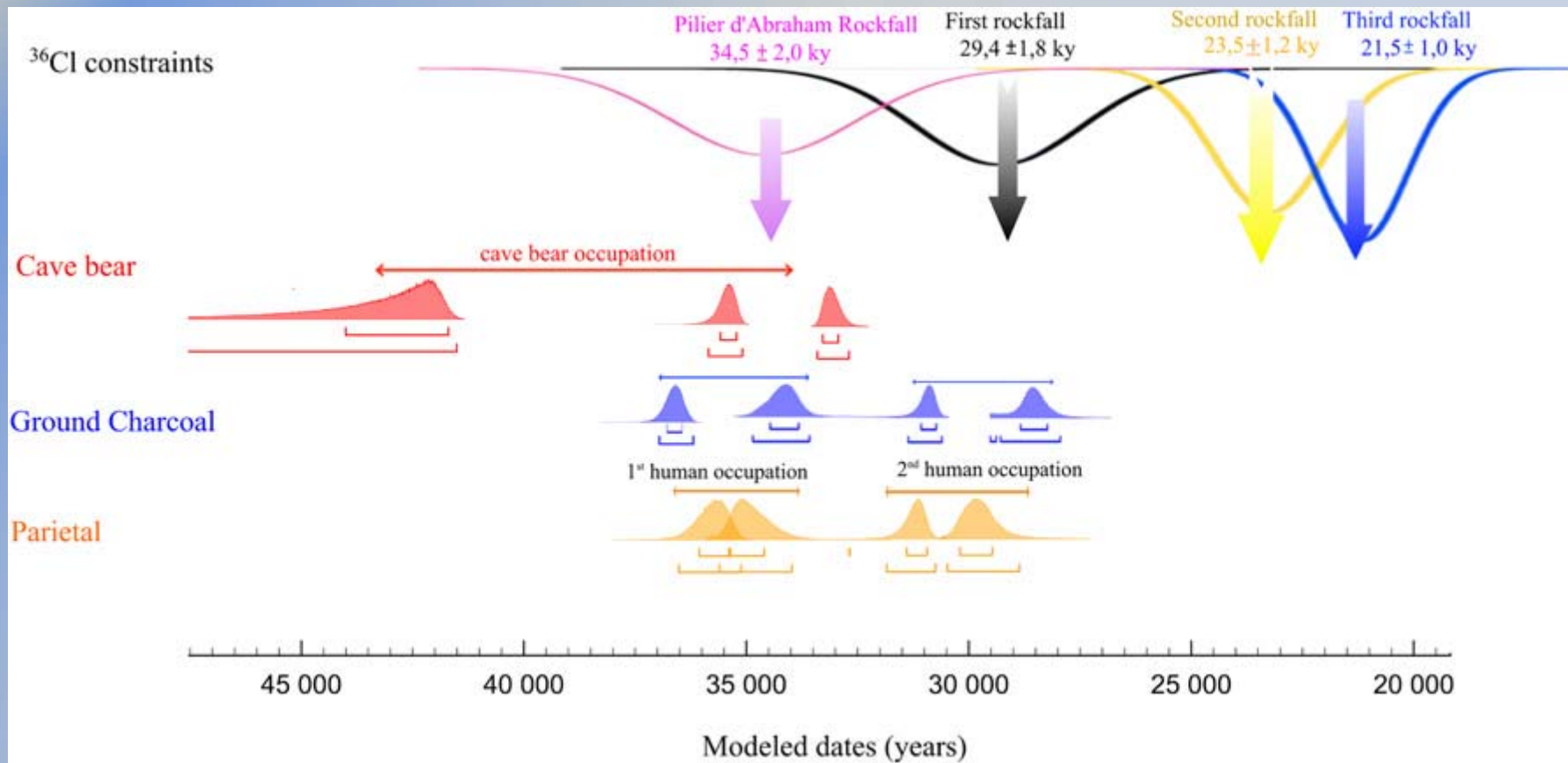
Bones

- Cave Bear Bone
- Other Species



0 10 20 30
Meters

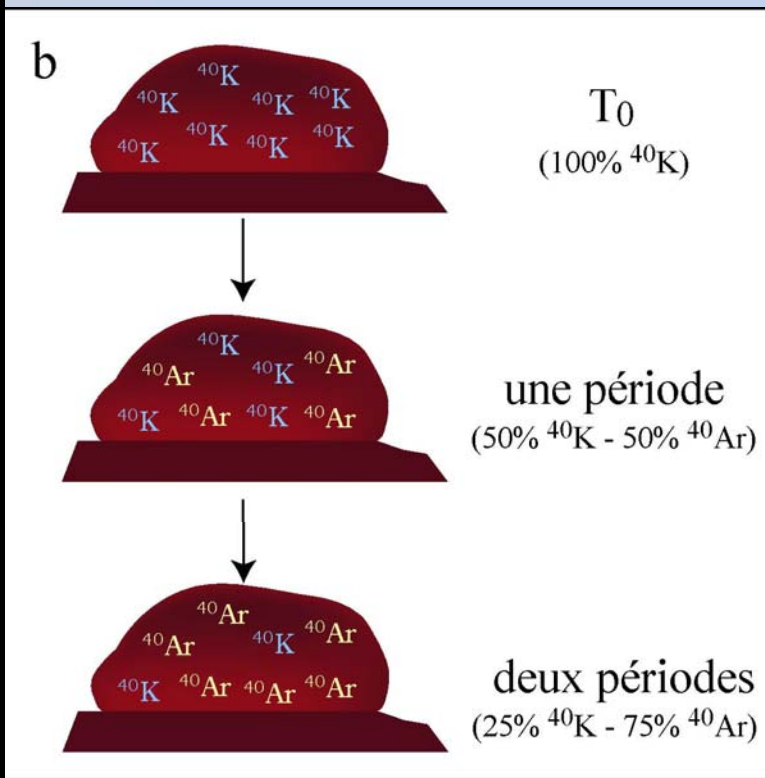
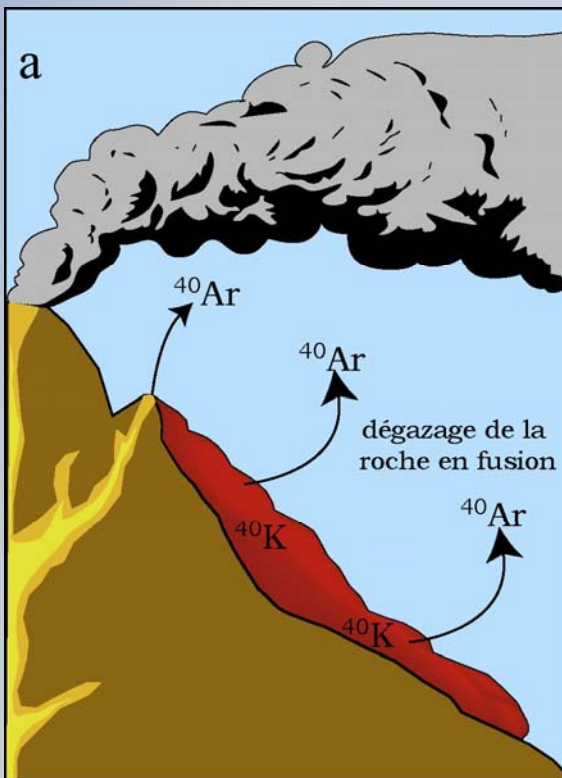
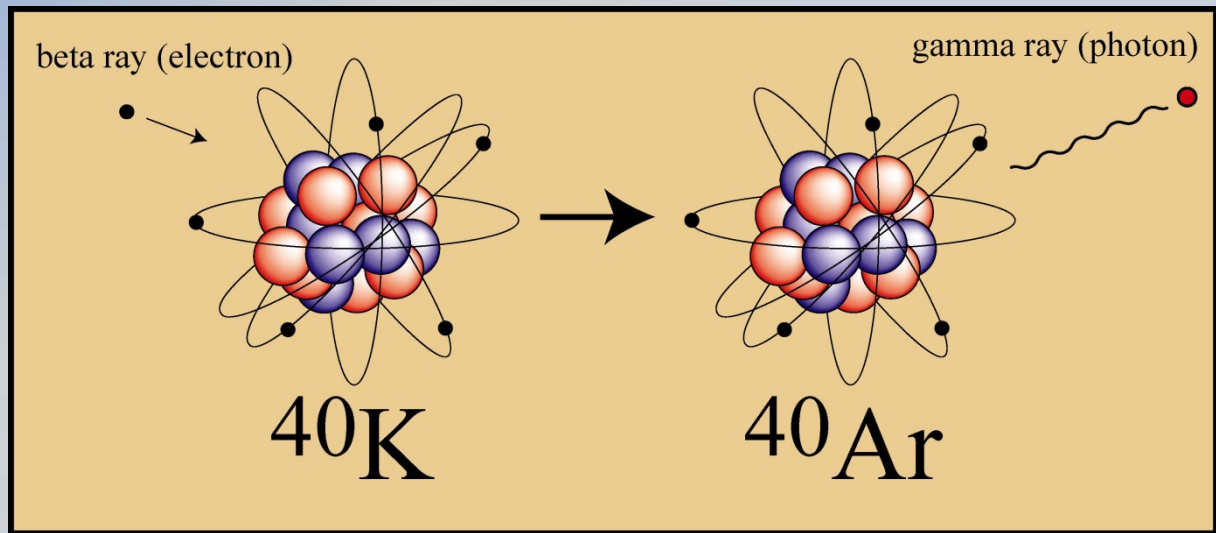




High-precision Bayesian model obtained for the Chauvet-Pont d'Arc Cave. Modeled boundaries for the start and end of each occupation phase are represented in red for the Cave Bear model (postulating a continuous occupation), in blue for the Cave Floor Charcoal model, and in orange for the Parietal model. Two distinct human occupations are clearly identified, extending from 37,000 to 33,500 y ago for the first one, and from 31,000 to 28,000 y ago for the second one. Cave bear presence in the cave is attested until 33,000 y ago. (Quiles et al., PNAS, 2016)

Argon methods

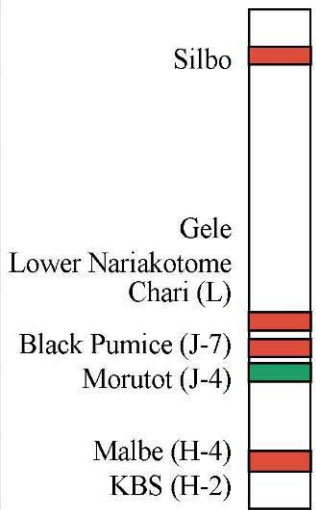




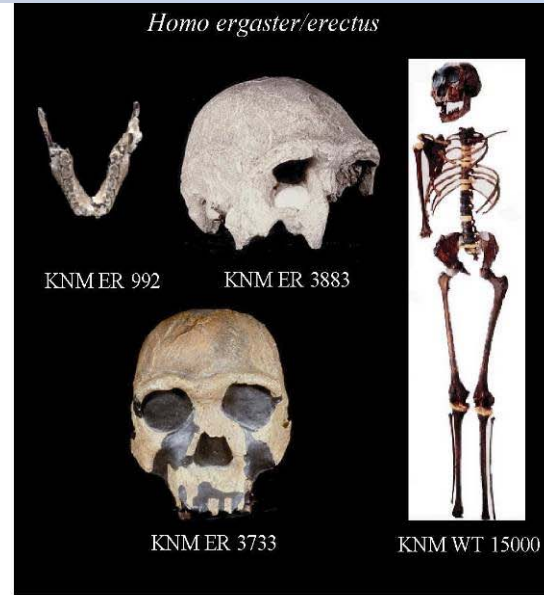
East Africa

Âges de quelques niveaux volcaniques du Bassin de l'Omo-Turkana (d'après Brown, 1994)

Age (Ma)



| | | |
|-----------------------------|--------------------|------------------------|
| Silbo | $0,74 \pm 0,01$ Ma | |
| Gele | $1,25 \pm 0,02$ Ma | |
| Lower Nariakotome Chari (L) | $1,33 \pm 0,03$ Ma | |
| | $1,39 \pm 0,02$ Ma | KNM ER 992 (1,50 Ma) |
| Black Pumice (J-7) | | KNM ER 3883 (1,55 Ma) |
| Morutot (J-4) | $1,65 \pm 0,03$ Ma | KNM WT 15000 (1,60 Ma) |
| Malbe (H-4) | $1,86 \pm 0,02$ Ma | KNM ER 3733 (1,80 Ma) |
| KBS (H-2) | $1,88 \pm 0,02$ Ma | KNM ER 1805 (1,85 Ma) |
| | | KNM ER 1470 (1,90 Ma) |
| | | KNM ER 1813 (1,90 Ma) |





Dmanisi site, Georgia
The first settlement out of Africa



5 skulls and 4 mandibles + post-cranial human remains associated to a Lower Pleistocene fauna and artefacts>



Struthio dmanisensis



Megantereon megartereon



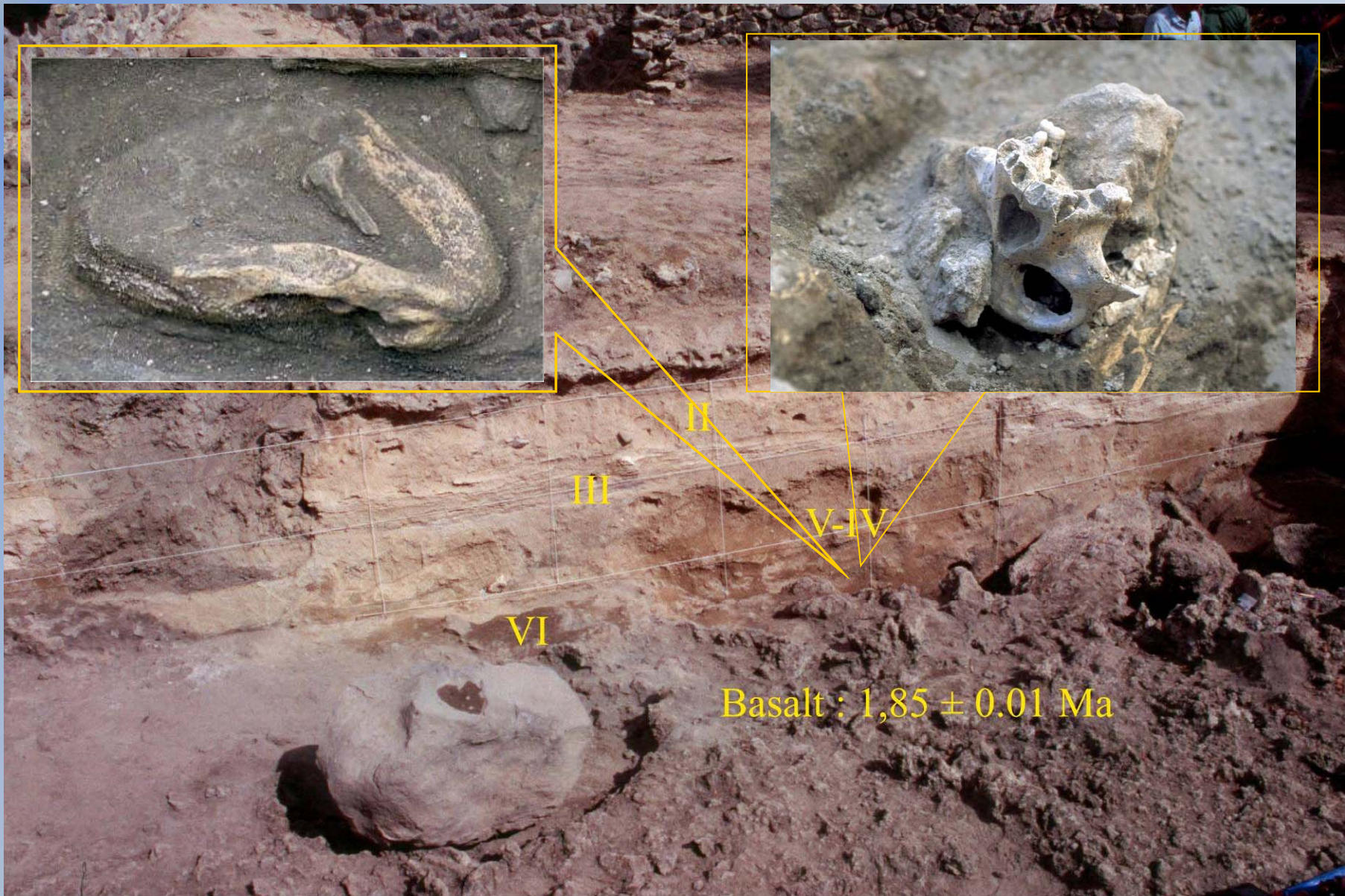
Archidiskodon meridionalis



Chopping Tool

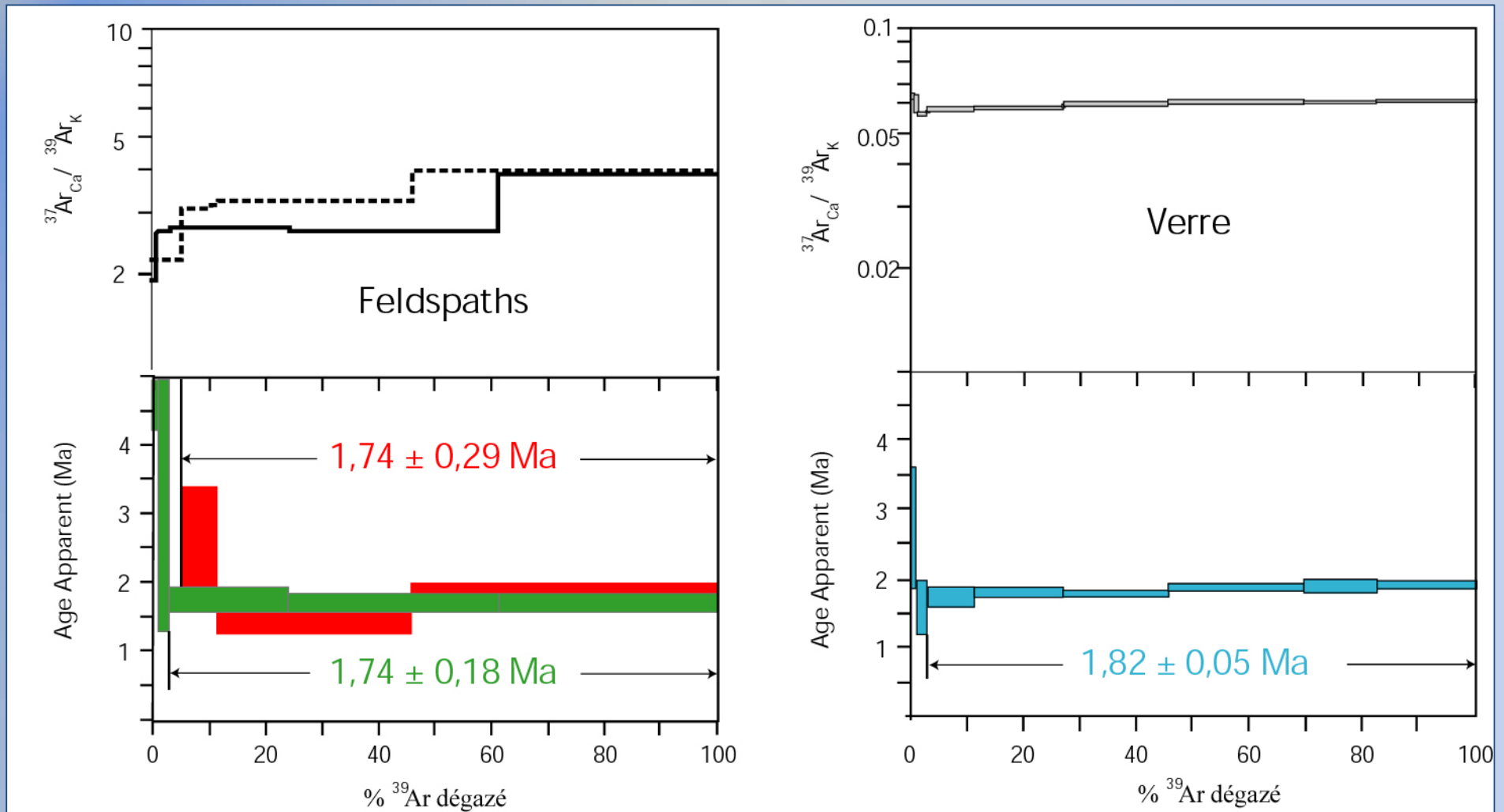


Chopper



Basalt : 1,85 ± 0.01 Ma

$^{40}\text{Ar}/^{39}\text{Ar}$ Age spectra on the D2600 mandible level



Weighted Mean : $1,81 \pm 0,05$ Ma
(Garcia et al., Quat Geochrono, 2010)



POMPEI et HERCULANUM, 79 AD

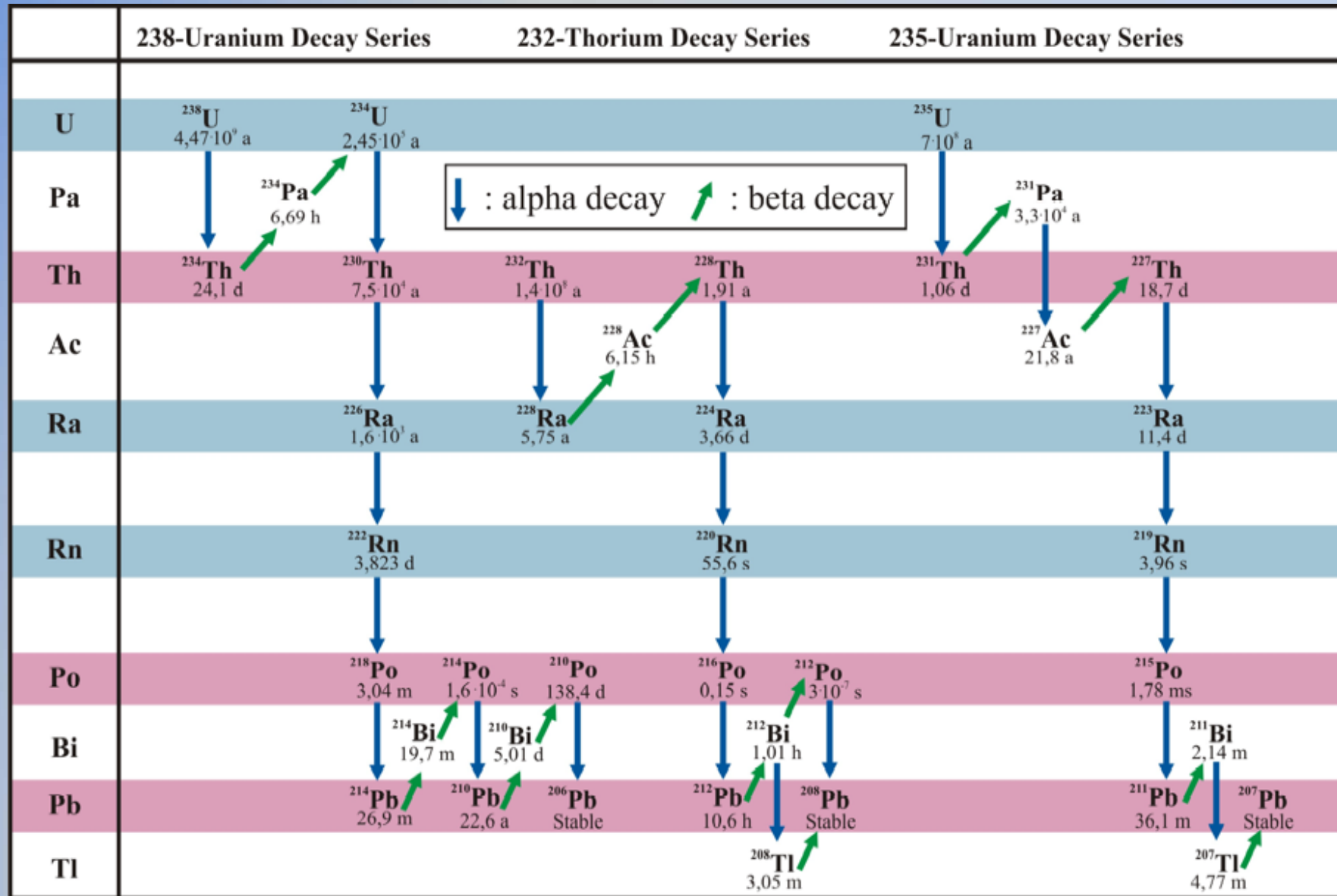
ISOCHRON $^{40}\text{Ar}/^{39}\text{Ar}$ AGE

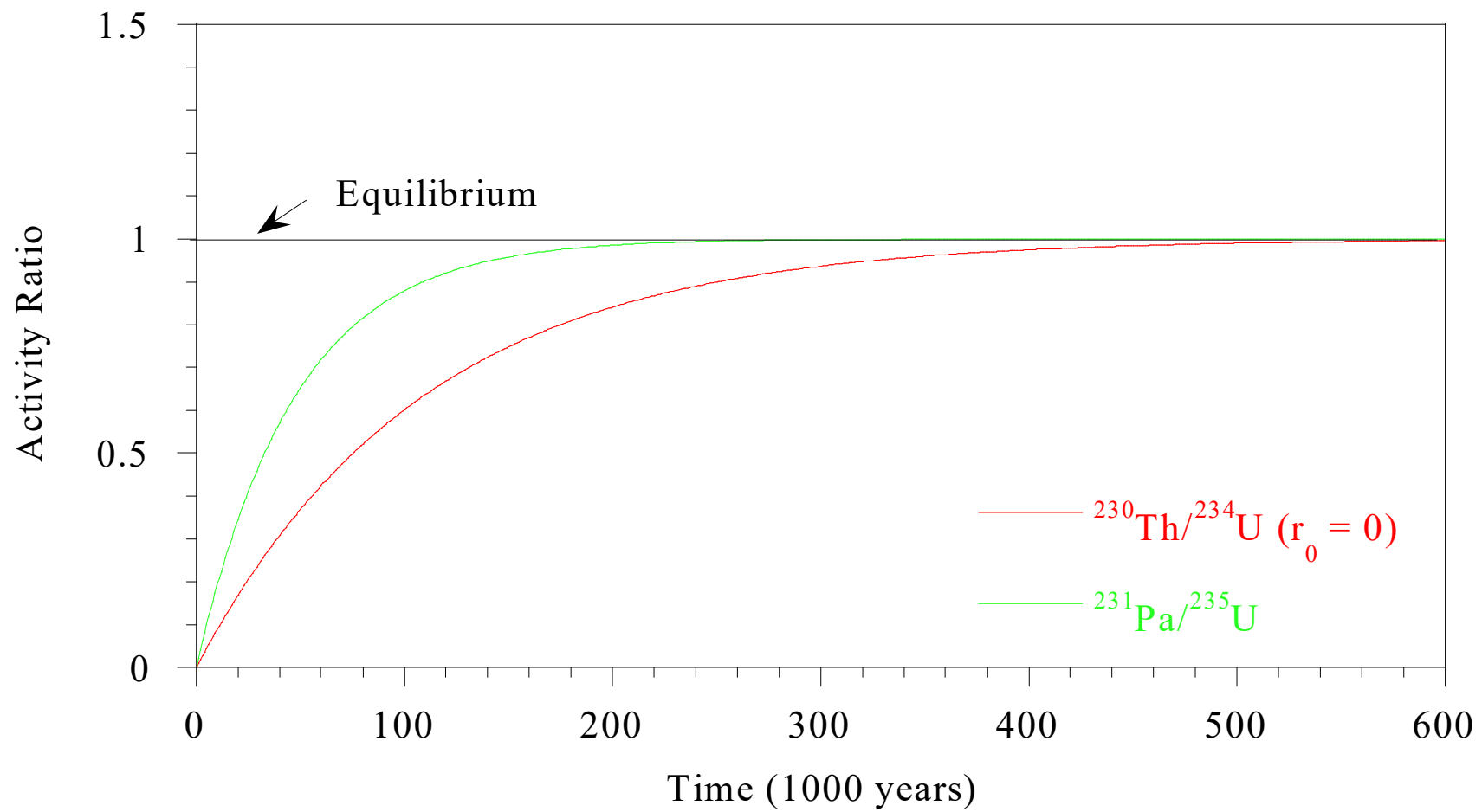
1925 ± 94 years (2 sigma error)



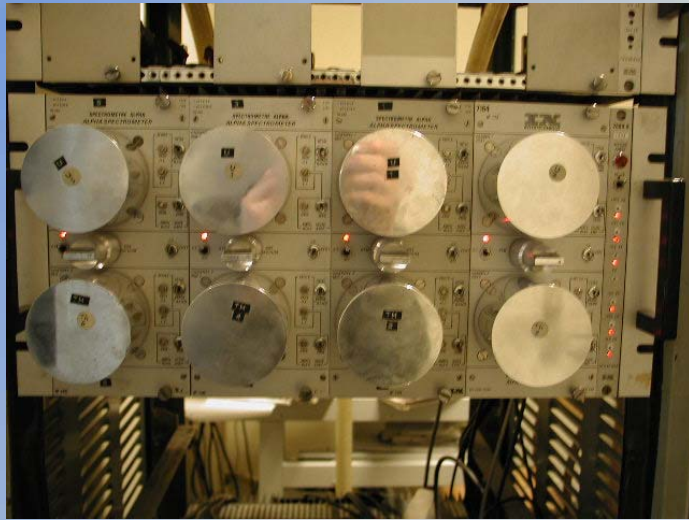
(Renne et al., *Science*, 1997)

Uranium-series methods





Activity measurement by alpha, gamma counting



$A_{238}, A_{234}, A_{230}, A_{232}$
[U] = 0.3 $\mu\text{g/g}$ \rightarrow
0.2 decay/mn



TIMS

Or measurement of N by
mass spectrometry
Atom measurement/second
Using the decay law

$$A = N \cdot \lambda$$

[U] = 0.3 $\mu\text{g/g}$ \rightarrow

$^{238}\text{N} = 8 \cdot 10^{14}$ atoms



ICPMS-MC

Alpha Spectrometry

Accuracy ~ 1 to 10%

1 μg U \Rightarrow 3 -10 g of carbonate

TIMS

Accuracy ~ 0.2-0.5%

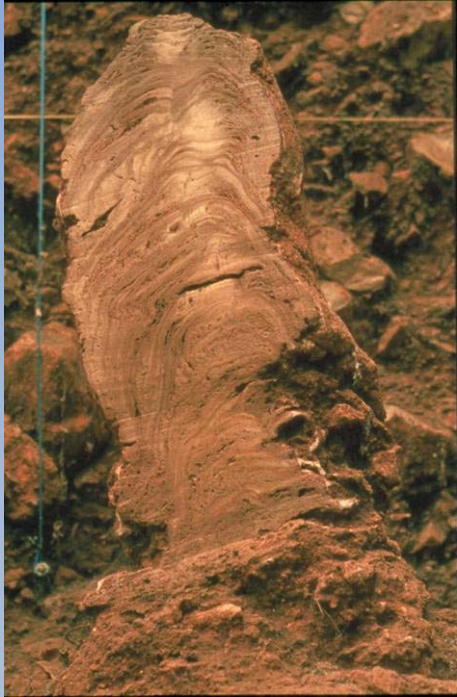
0.2 μg U \Rightarrow 0.5 g of carbonate

Laser Ablation – MC-ICPMS – ICP-QMS

Accuracy ~ 0.1-0.5%

0.05 -0.2 μg U \Rightarrow 0.1-0.5g of carbonate

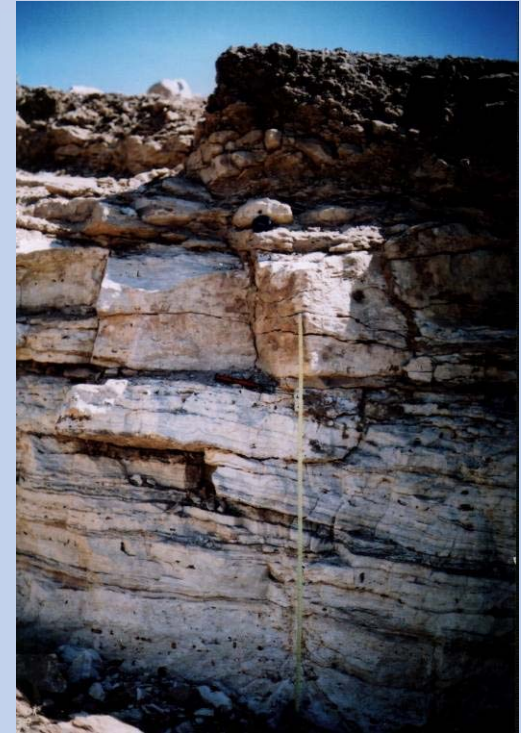
CONTINENTAL CARBONATES



Stalagmite



Stalagmitic floor

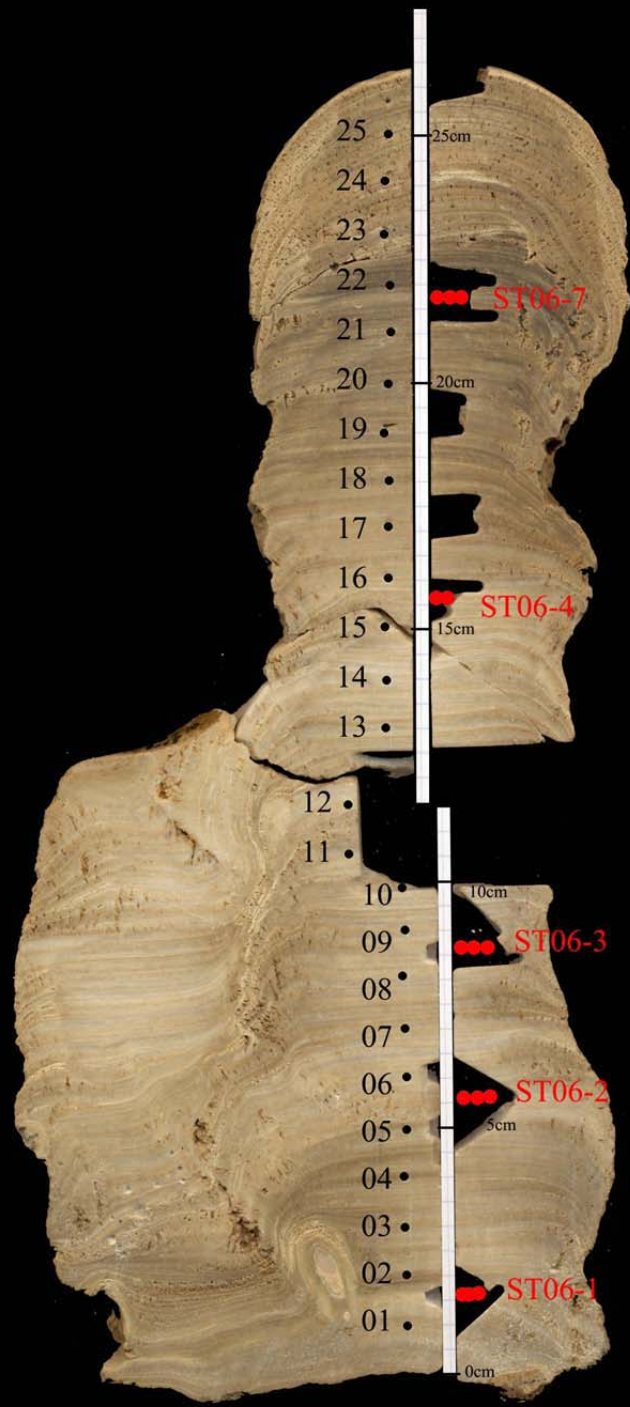
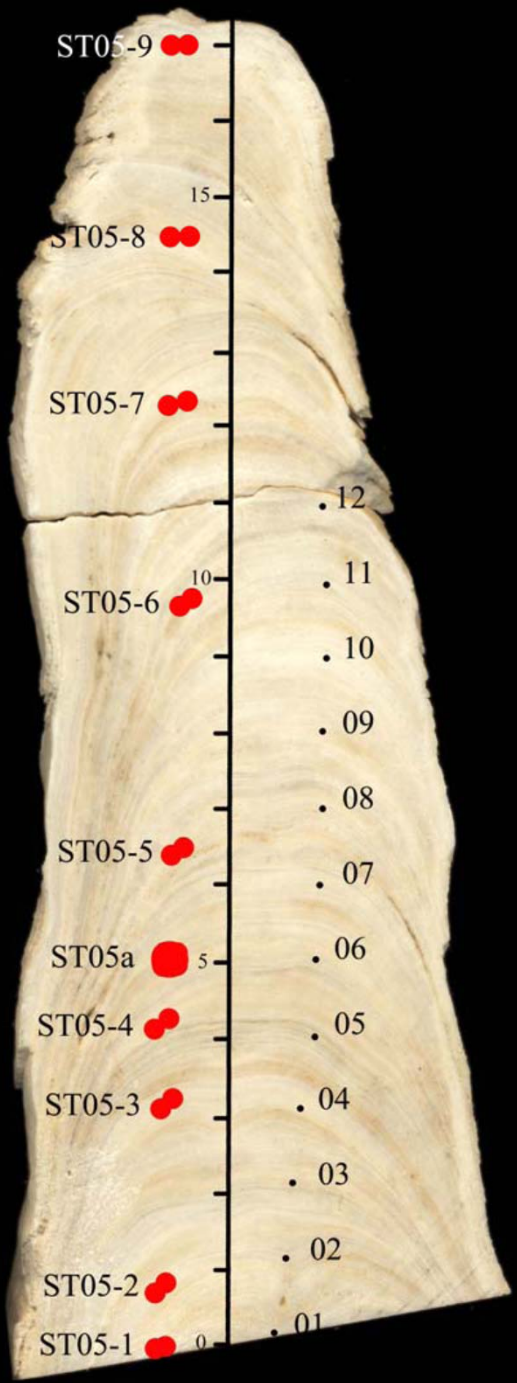


Travertines

Dating prehistoric sites in karstic area by uranium-series

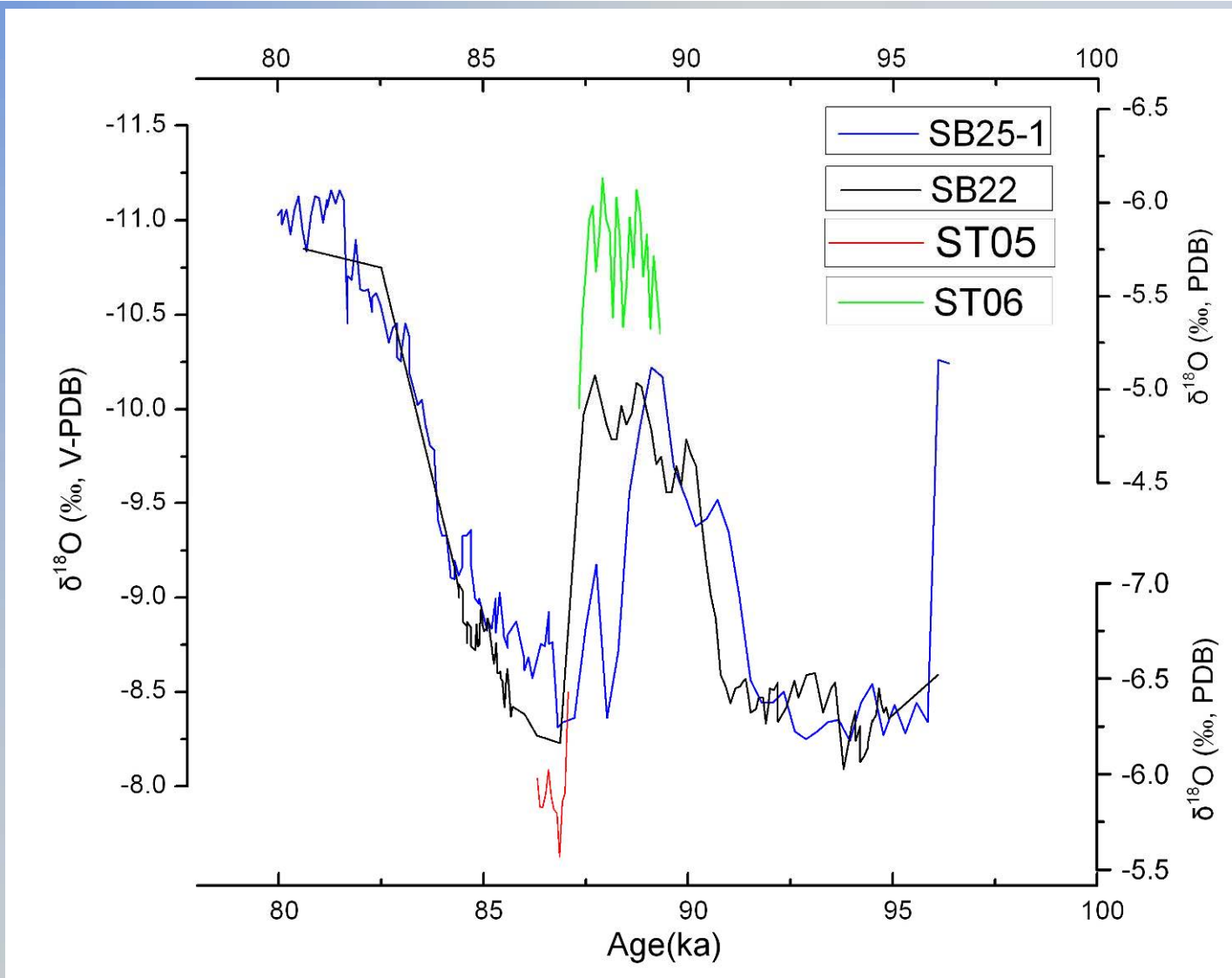


Song Terus and Tabuhan caves,
Java, Indonesia



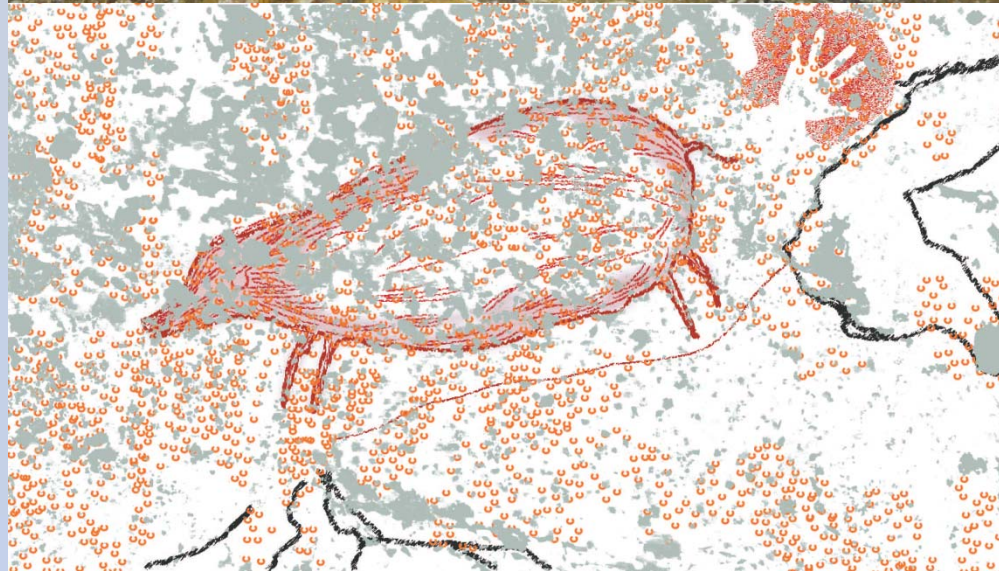
| | 238U | 234U/238U | 230Th/238U | 230Th/232Th | Age[ka] |
|---------------|-------------|---------------------------|---------------------------|-------------|------------------------|
| ST06-1 | 1.12 | 1.1398±0.0011 | 0.6557±0.0021 | 98.93 | 91.4±0.5 |
| ST06-2 | 1.33 | 1.1406±0.0010 | 0.6050±0.0018 | 287.49 | 80.9±0.4 |
| ST06-3 | 1.14 | 1.1407±0.0013 | 0.6349±0.0030 | 152.45 | 86.9±0.6 |
| ST06-4 | 1.16 | 1.1412±0.0026 | 0.6224±0.0023 | 204.11 | 84.3±0.6 |
| ST06-7 | 1.21 | 1.1428±0.0008 | 0.6291±0.0028 | 94.46 | 85.5±0.6 |
| ST05-1 | 2.99 | 1.1168±0.0012 | 0.6319±0.0015 | 2052.60 | 89.4±0.4 |
| ST05-2 | 3.50 | 1.1183±0.0010 | 0.6259±0.0025 | 10986.67 | 87.99±0.5 |
| ST05-3 | 3.61 | 1.1127±0.0009 | 0.5962±0.0012 | 4845.07 | 82.43±0.3 |
| ST05-4 | 3.64 | <i>1.1177±0.0015</i> | <i>0.9374±0.0034</i> | 2866.72 | <i>186.8±1.8</i> |
| ST05-5 | 2.40 | <i>1.1116±0.0009</i> | <i>0.6882±0.0016</i> | 1539.94 | <i>103.1±0.4</i> |
| ST05-a | 3.48 | <i>1.103±0.020</i> | <i>0.529±0.016</i> | 345 | <i>80.9±3.8</i> |
| ST05-6 | 3.53 | 1.1086±0.0009 | 0.6187±0.0044 | 4510.04 | 87.6±0.9 |
| ST05-7 | 4.54 | 1.1066±0.0005 | 0.6005±0.0012 | 2596.66 | 84.4±0.2 |
| ST05-8 | 3.58 | 1.1055±0.0007 | 0.6304±0.0022 | 4196.88 | 90.6±0.5 |
| ST05-9 | 3.65 | 1.1030±0.0007 | 0.6203±0.0014 | 9352.38 | 88.7±0.3 |

(TU Hua., M2 Master, 2012, unpublished data)

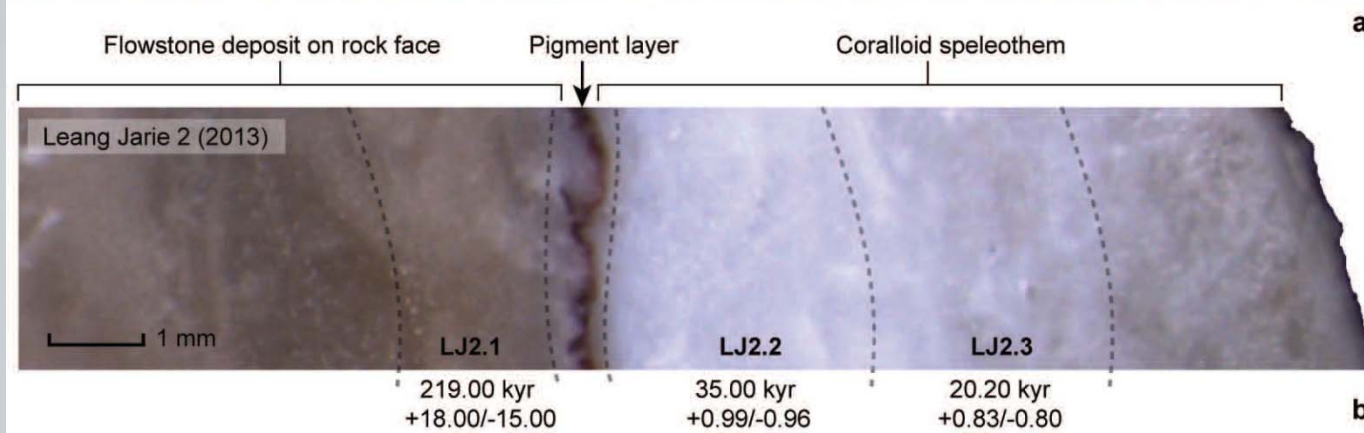
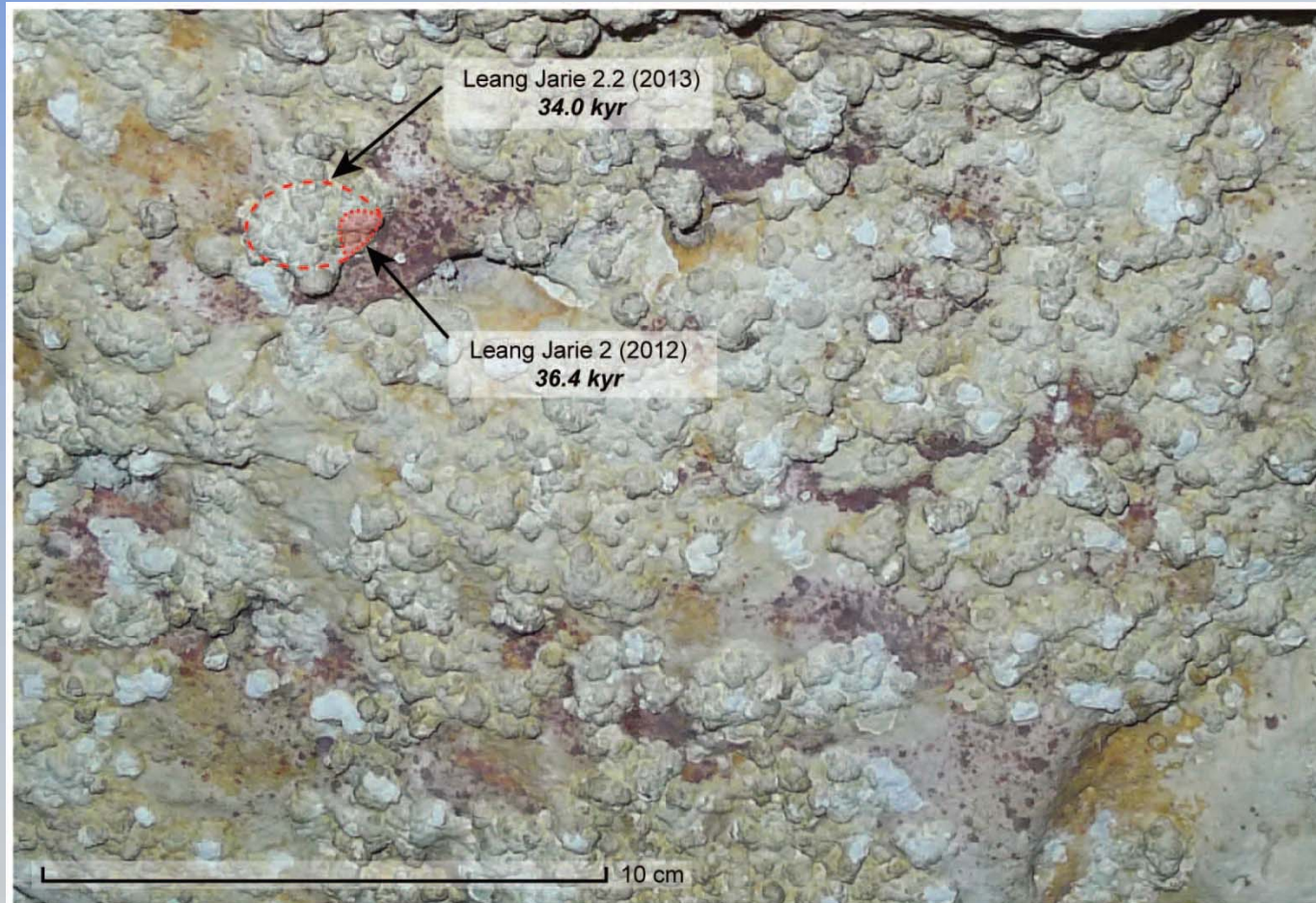


Comparison of isotopic records between Song Terus and Sanbao caves within around 95-80 ka. The left vertical axis corresponds to Sanbao curves, and the right ones are for ST06 (top) and ST05 (down).

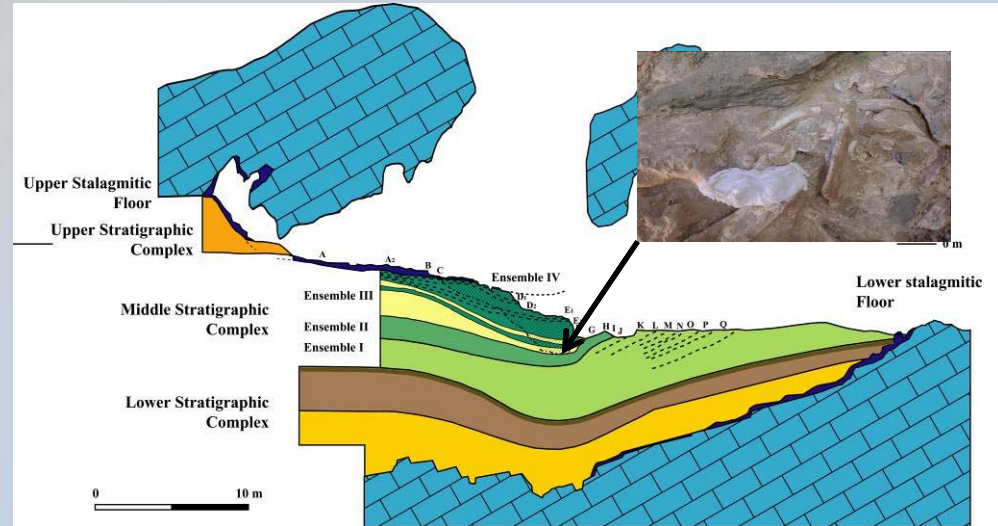
Dating valuable paintings in Sulawesi, Indonesia



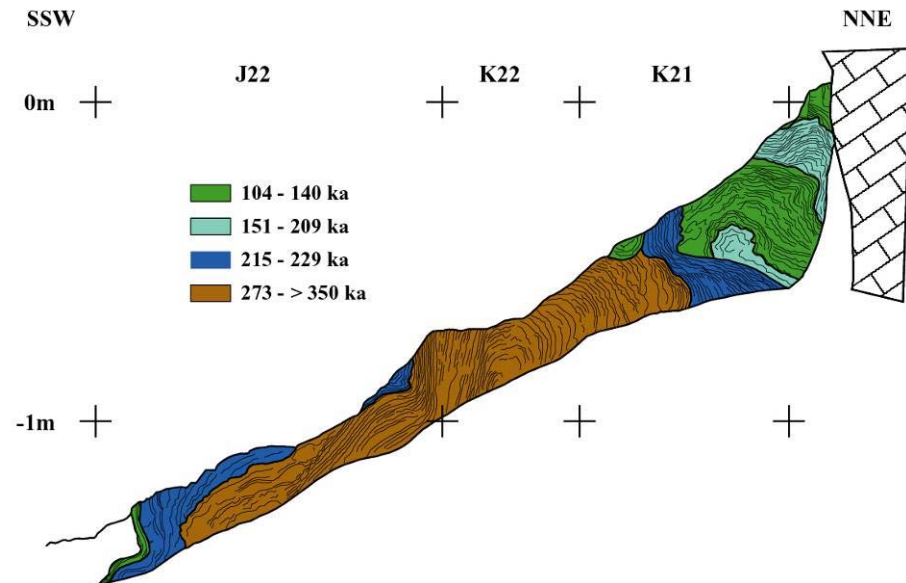
(Aubert et al., Nature, 2014)

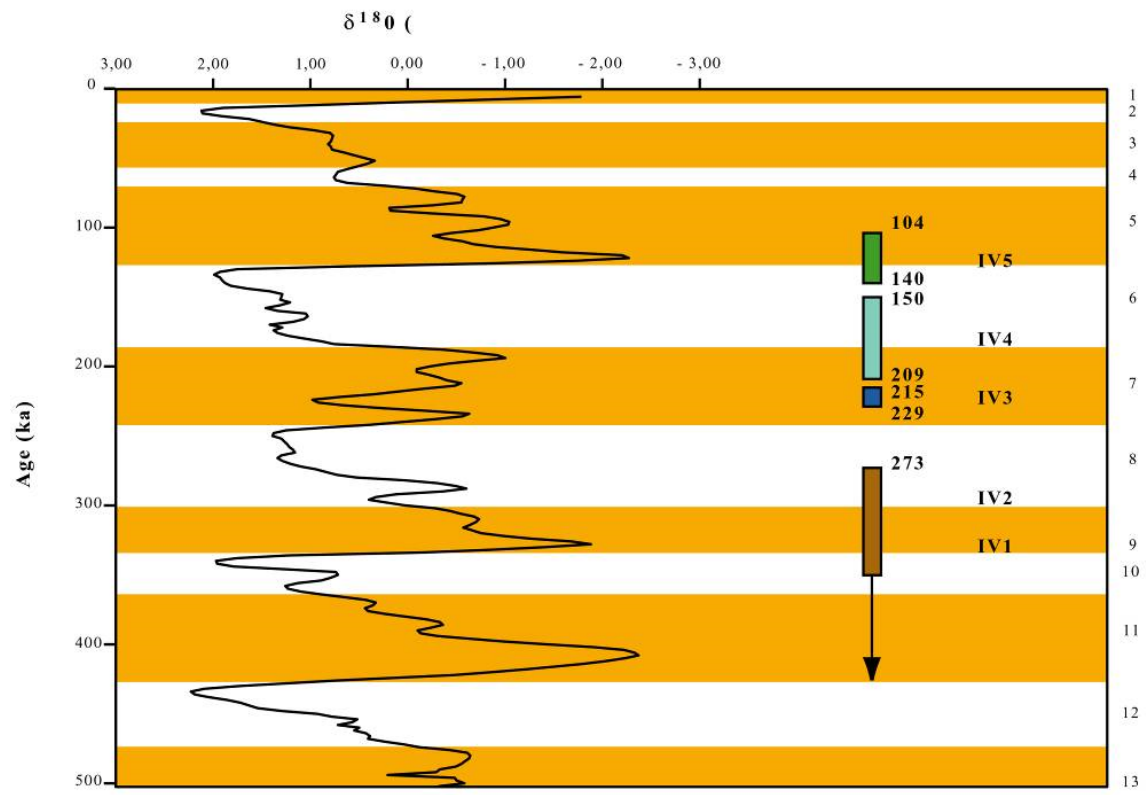


ARAGO CAVE, FRANCE

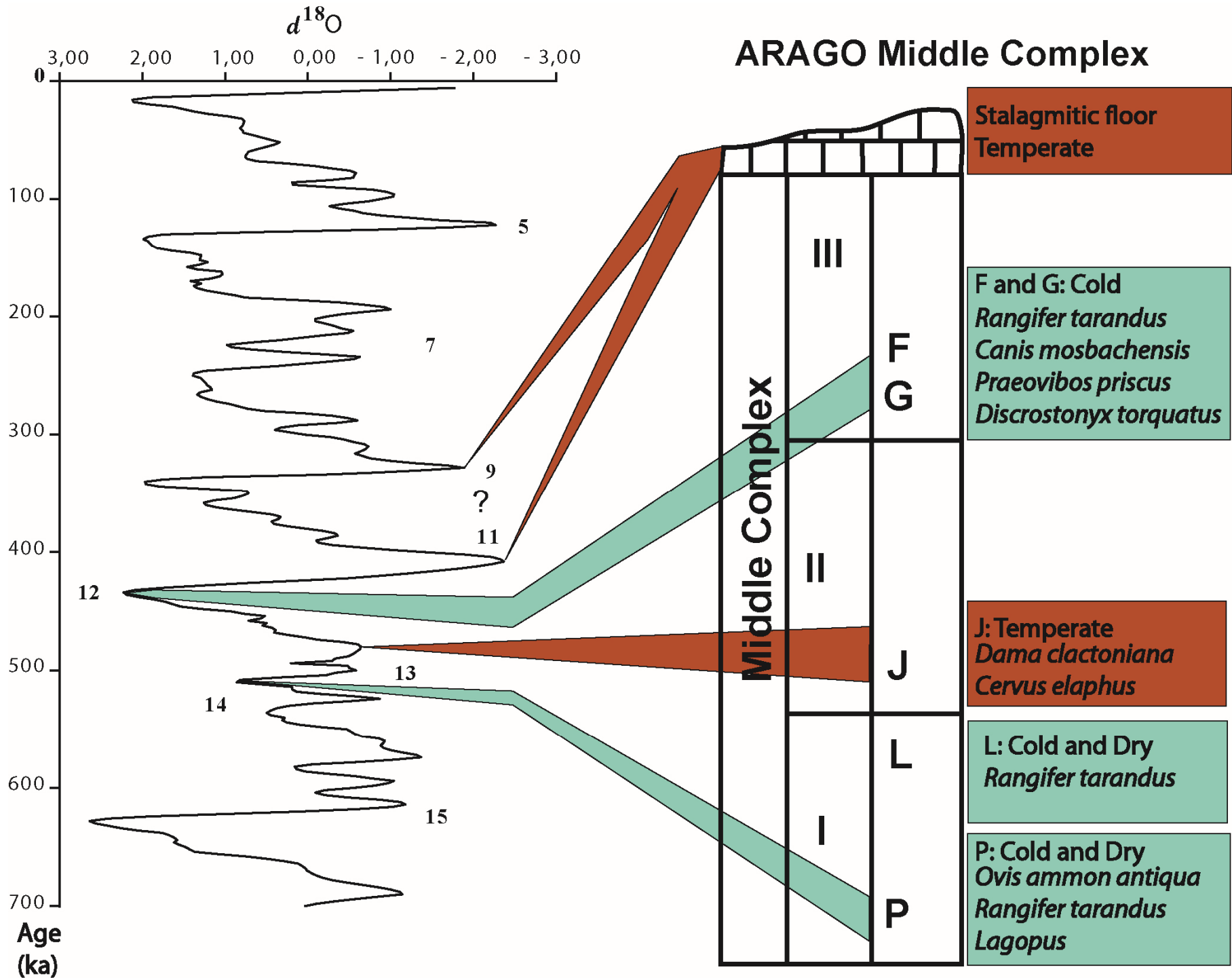


Uranium-Thorium - applications - Datation de la Caune de l'Arago





ARAGO Middle Complex



MARINE CARBONATES



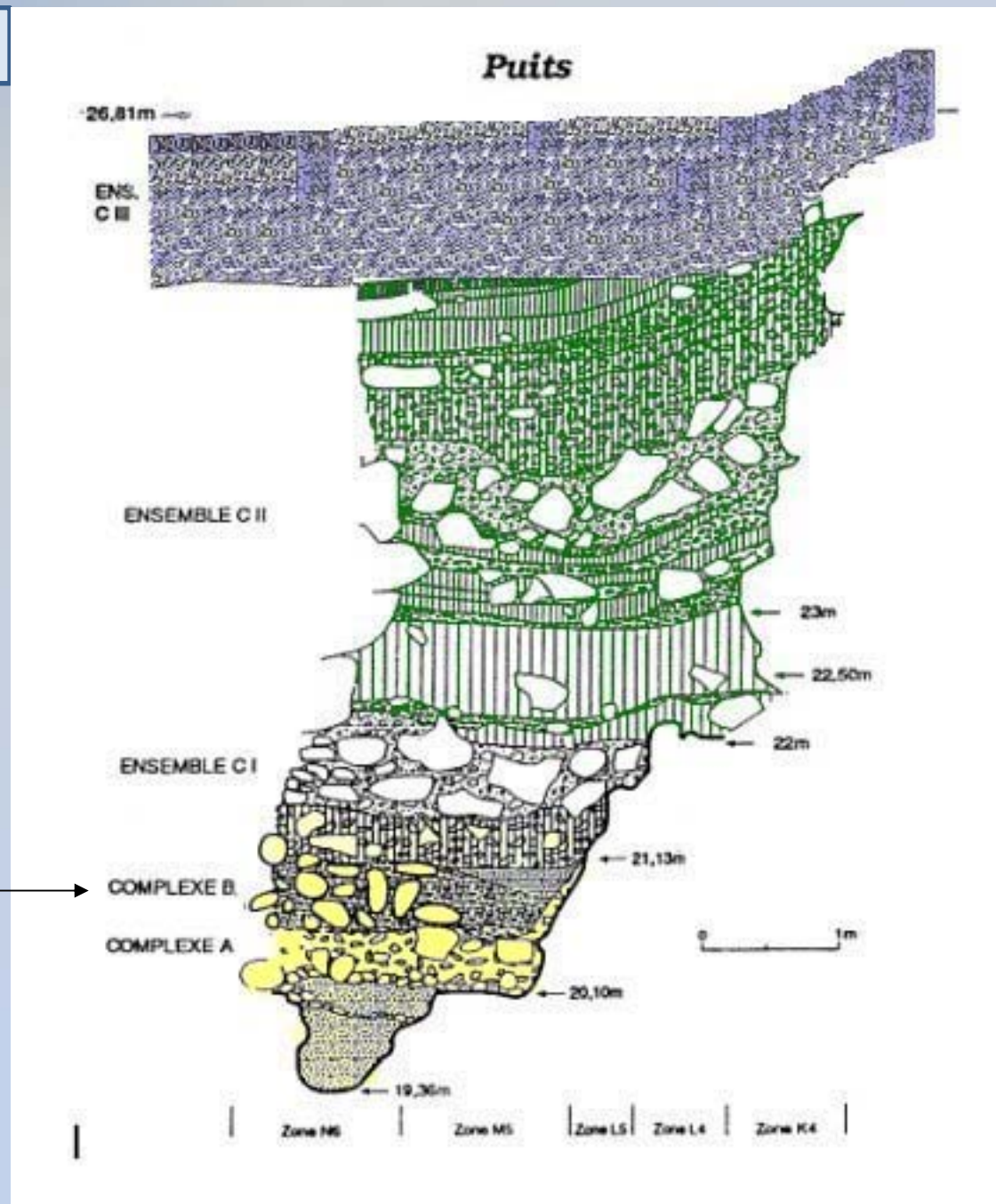
Shells and corals



LAZARET CAVE, NICE, FRANCE

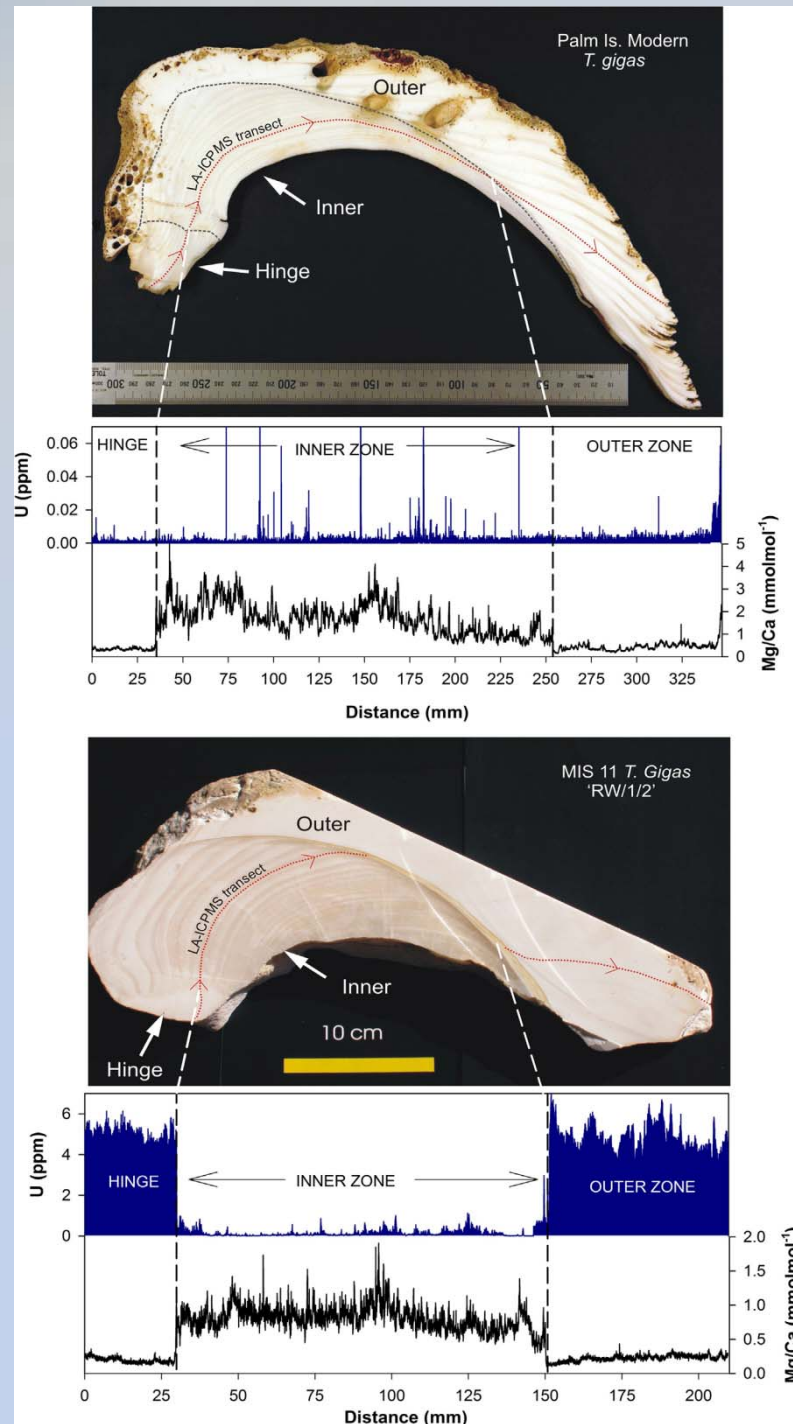


238 +22/-18 ka
Corals



Profiles of uranium concentrations in modern and MIS 11 *T. gigas* specimens, spanning the hinge, inner and outer zones (data acquired using LA-ICPMS). (Ayling et al., GCA, 2017)

Zonal differences in U concentration are attributed to crystallographic differences between the growth zones, which are likely to affect the specific surface area of the aragonite crystal lattice and thus the availability of surface binding sites for uranium adsorption.



Cosmogenic isotopes

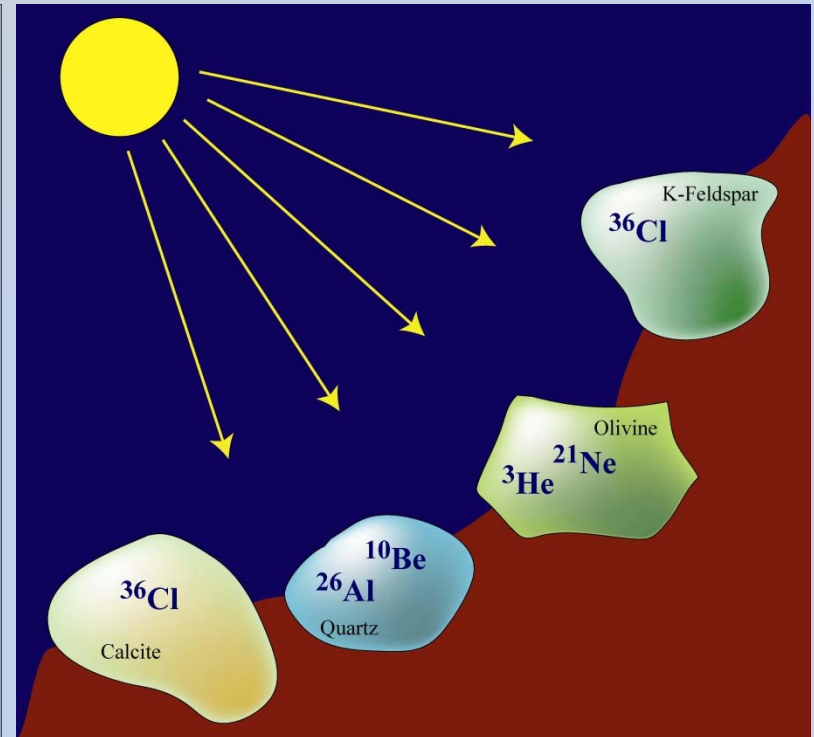
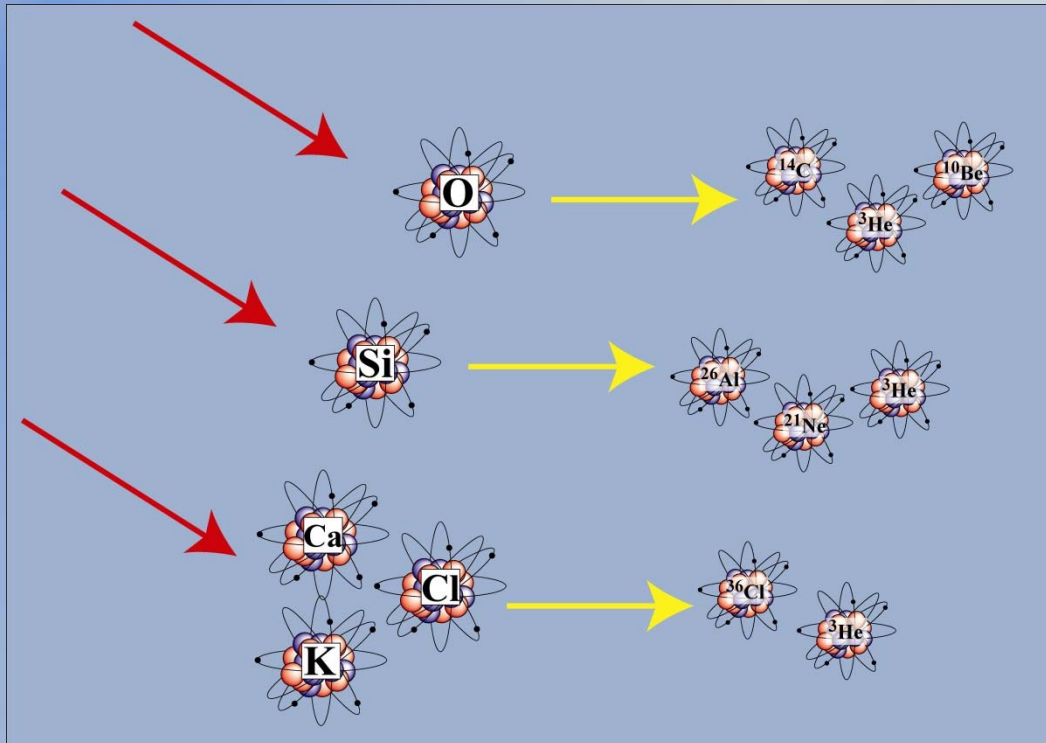
The dating of exposure by cosmogenic isotopes is a geochemical dating method which uses the production of rare isotopes by the cosmic rays, then their accumulation in the minerals crystal lattice to determine an exposure age.

In paleosismology, to date a surface shifted by a fault.

In geomorphology, to calculate erosion rates :
by using a couple of isotope and their respective half-life.

In geomorphology, to obtain the age of an alluvial terrace, a moraine or any other formation.

In paleoglaciology, to estimate a deglaciation :
the exposure starts when the ice does not cover any more the rock.

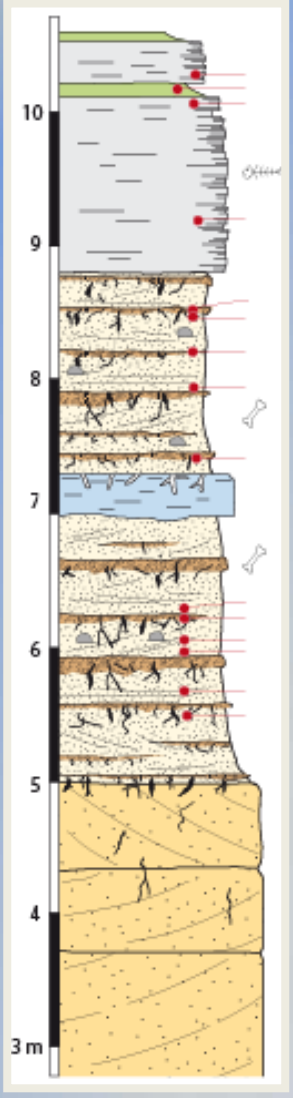


For instance, helium (4He), Beryllium (^{10}Be), aluminium (^{26}Al), chlorine (^{36}Cl), carbon (^{14}C), neon (^{21}Ne)

The isotopes production rates depend on:

- Altitude
- Latitude
- Depth (thickness of rock, water and/or snow to the top of the sample)
- Angle of incidence (angle enters the vertical and the sample)
- Masking related to topography (cliff, mountain...)

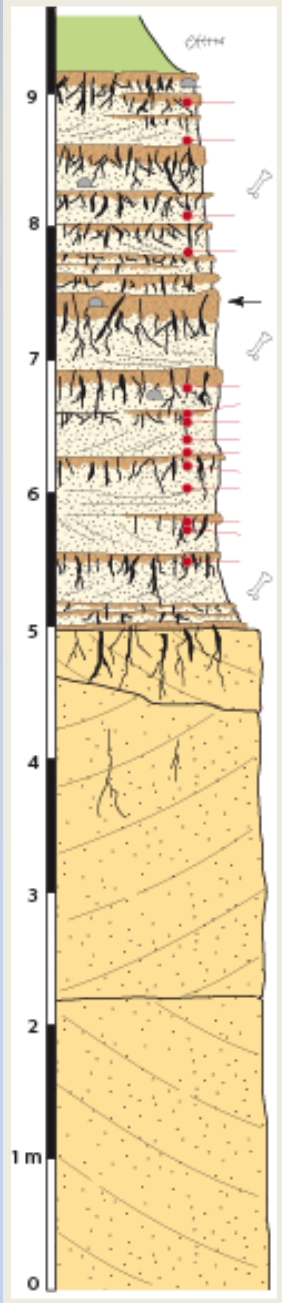
LACUSTRINE FACIES
 ANTHRACOTHERIID UNIT
 AEOLIAN FACIES



TM 254

6.25±0.15Ma
 7.13±0.14Ma
 7.46±.13Ma

TM 266



7.10±0.14Ma
 7.34±0.12Ma

S. tchadensis
 Holotype, cranium

Dating Toumai, Tchad

$^{10}\text{Be} : T_{1/2} = 1,4 \cdot 10^6 \text{ ans}$
 Authigenic $^{10}\text{Be}/^9\text{Be}$

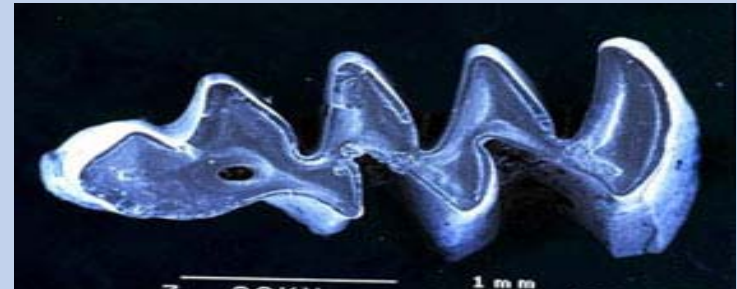


Sahelanthropus tchadensis
 about 7 Ma

(Lebatard et al., PNAS, 2008)

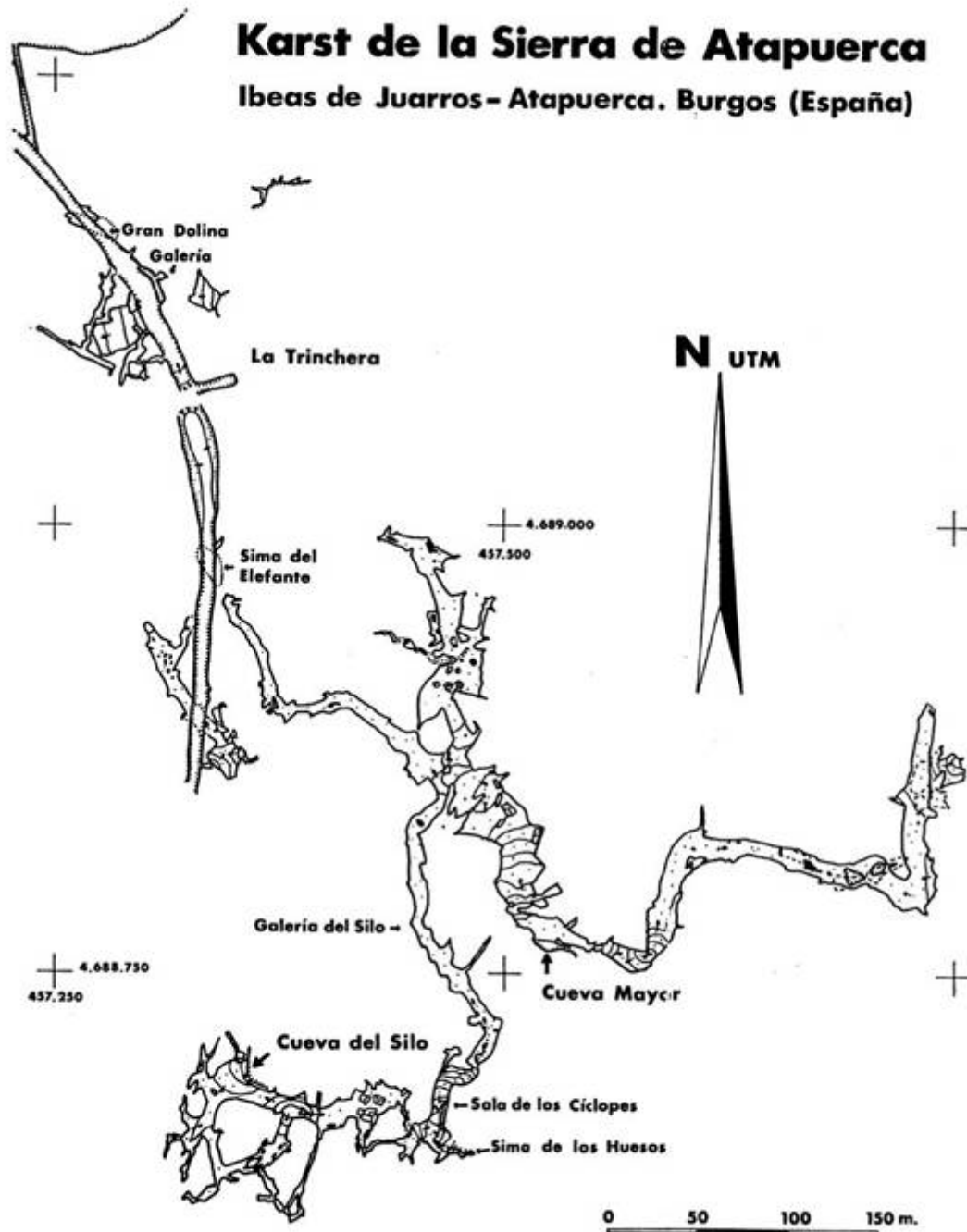


Sierra de Atapuerca, Espagne



Karst de la Sierra de Atapuerca

Ibeas de Juarros- Atapuerca. Burgos (España)



G. E. Edelweiss



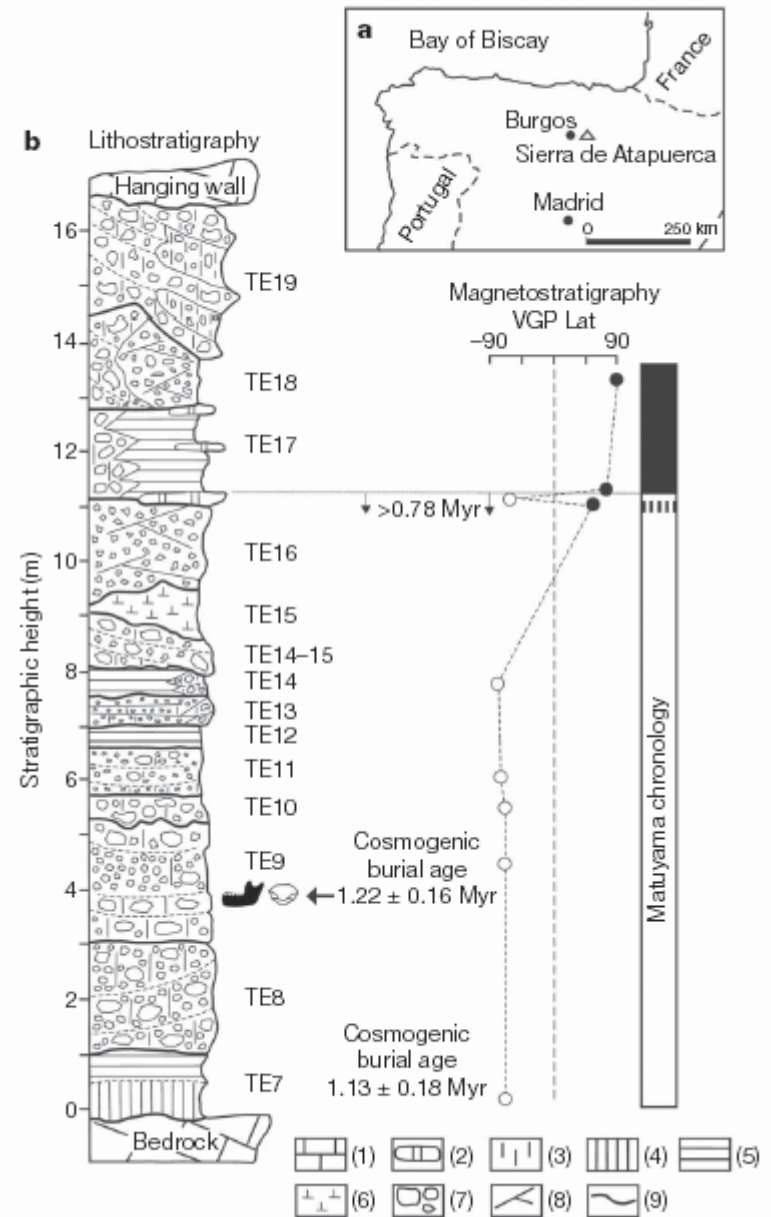
Lám. XVIII.—Entrada a la cueva de Atapuerca, en Ibeas de Juarros.



Sima del Elefante



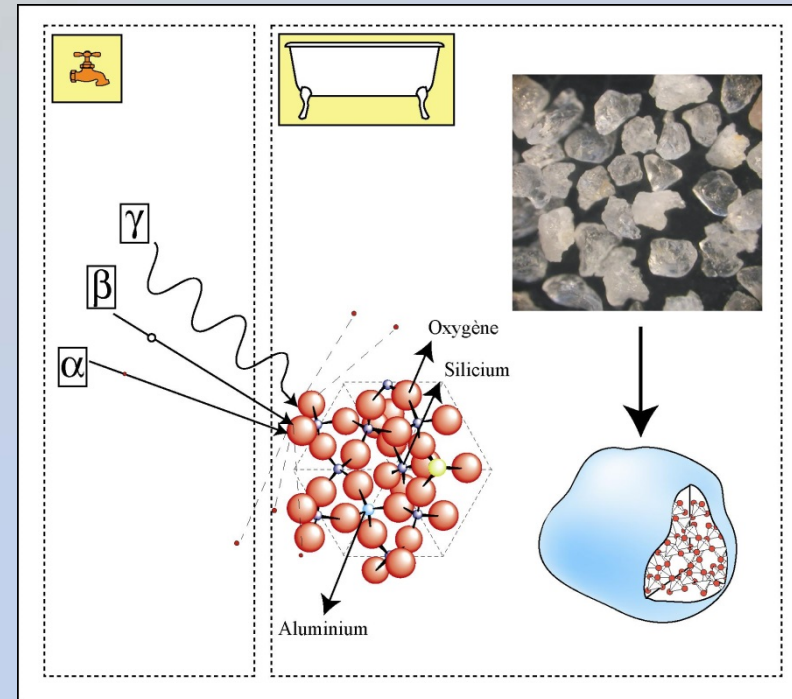
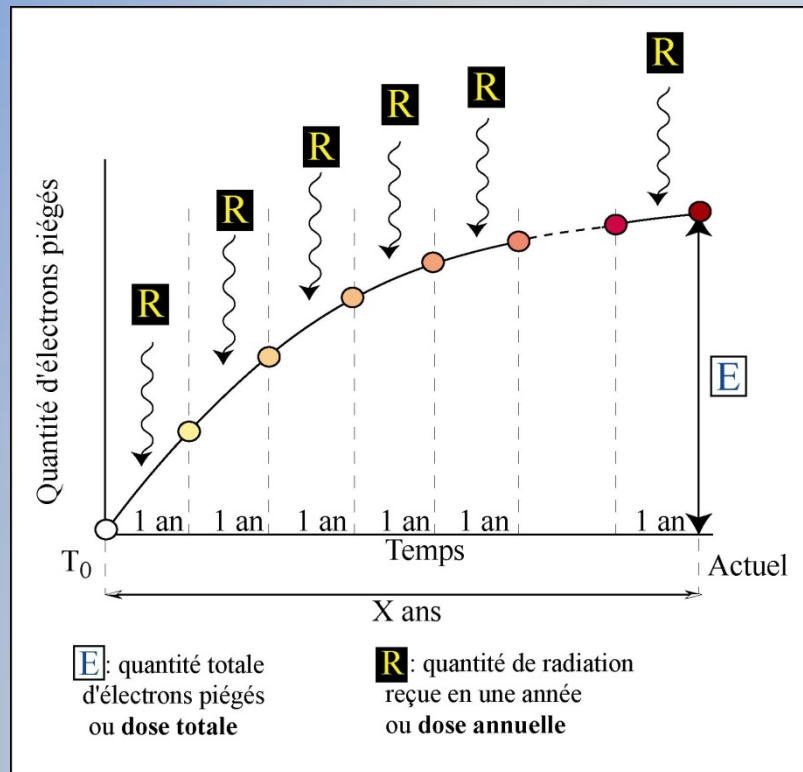
(Carbonell et al., Nature, 2008)



Palaeodosimetric Methods

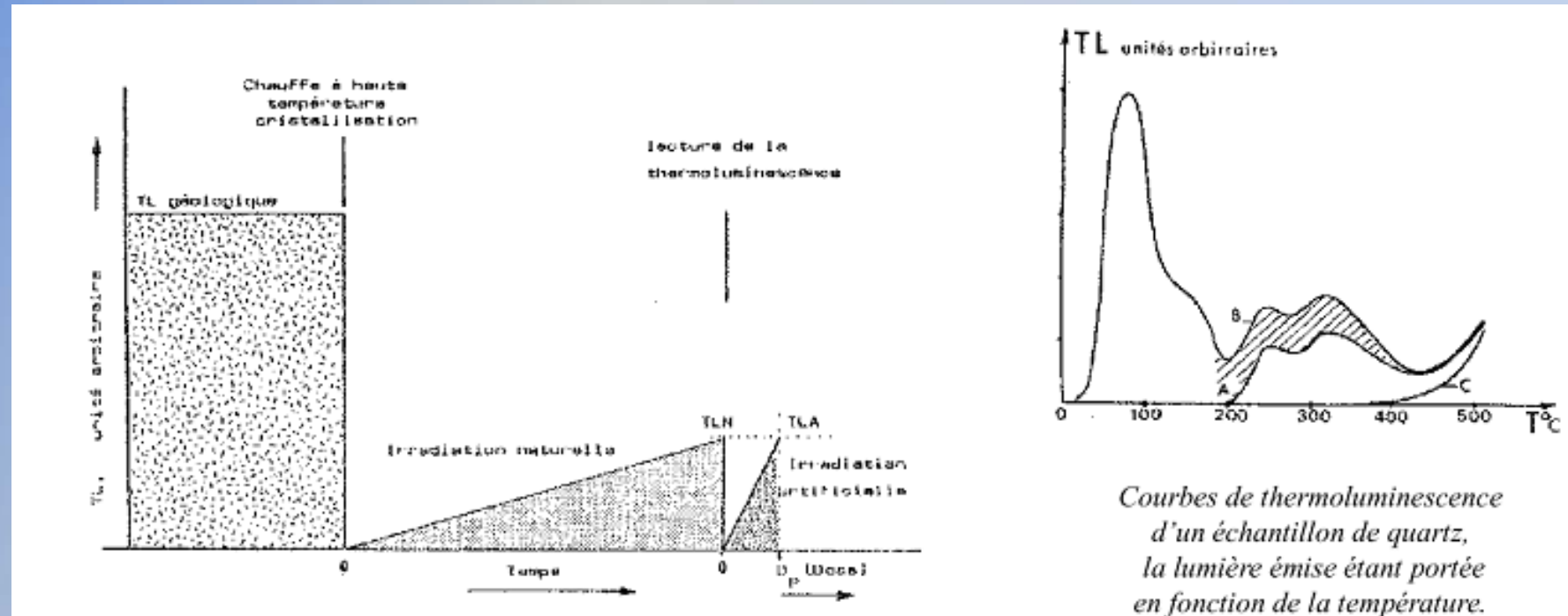
Résonance de Spin Électronique

Méthodes de la Luminescence



$$X \text{ ans} = \text{Age} = \frac{E}{R}$$

Thermoluminescence



Last dated event = last heating
or light exposure

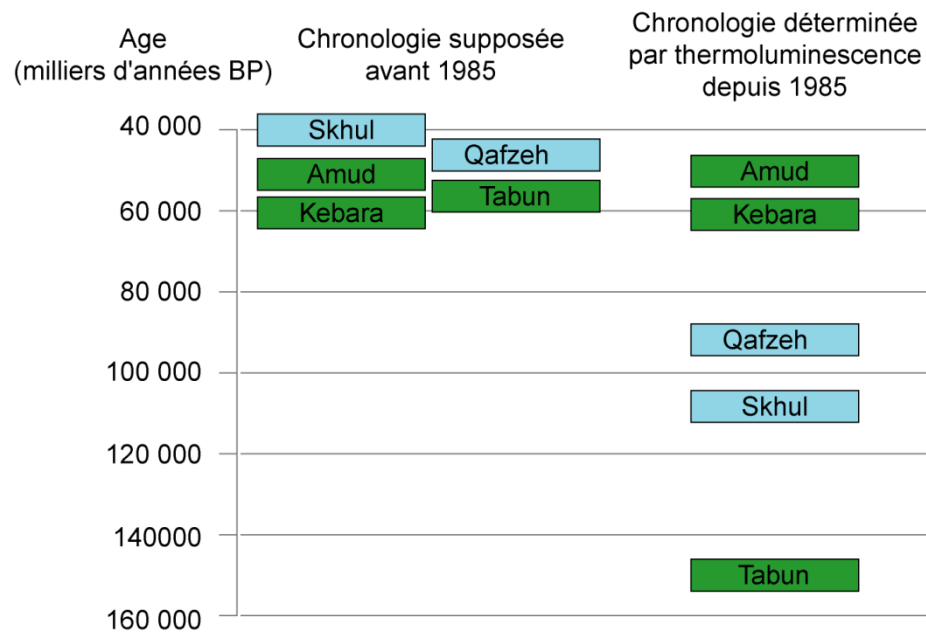
Main dating samples : burnt
flint, quartz, feldspar



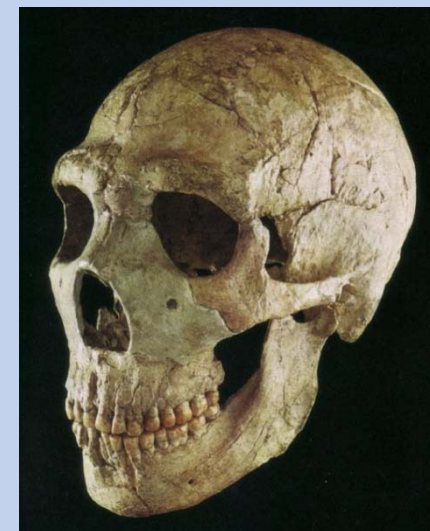
- Sites à néandertaliens
- Sites à Hommes modernes



Qafzeh 6



Application - Les sites à néandertaliens et hommes anatomiquement modernes du Levant



AMUD

Valladas et al., Nature, 1987

OSL

Optically Stimulated Luminescence

Last dated event = last light
exposure

Main datable samples :
quartz, feldspars

Applicability

OSL: Holocene, Upper Pleistocene

IRSL: Holocene Upper and Middle Pleistocene

TT OSL: Lower and Middle Pleistocene

PostIr-Ir: Lower and Middle Pleistocene

Cantera de las Torcas

LA TRINCHERA

Penal **Gran Dolina Galería**

Cueva del Compresor

Sima del Elefante

Cueva Peluda

Galería Baja

4.689.000
457.500

G. de las Estatuas

G. Principal /
Salón del Coro

Galería del Silo

4.688.750
457.250

Cueva del Silo

Portalón

Cueva Mayor

Sala de los Cíclopes

Sima de los Huesos



N
UTM

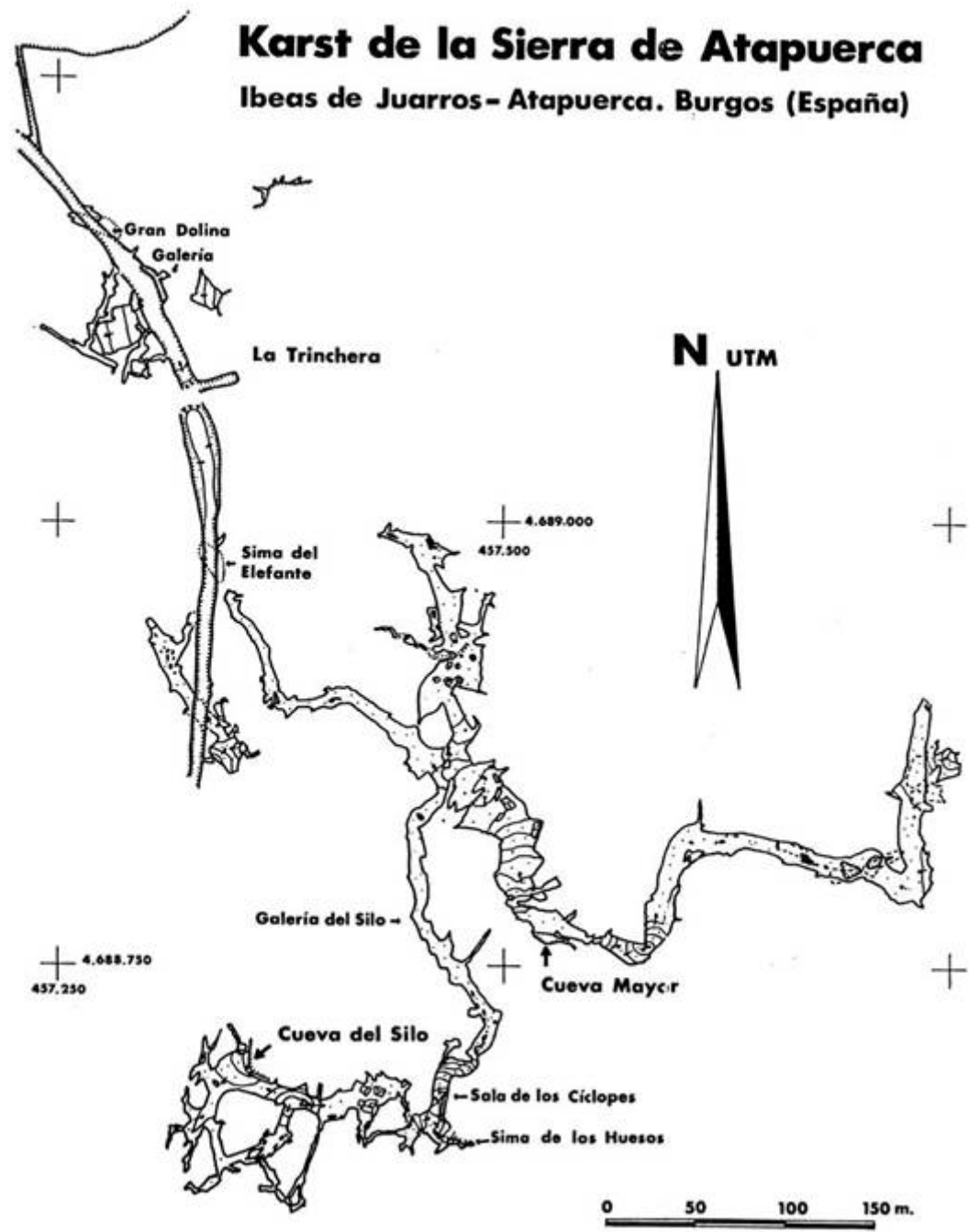


0 50 100 150m

G.E. Edelweiss

Karst de la Sierra de Atapuerca

Ibeas de Juarros - Atapuerca. Burgos (España)



G. E. Edelweiss



Lám. XVIII.—Entrada a la cueva de Atapuerca, en Ibeas de Juarros.

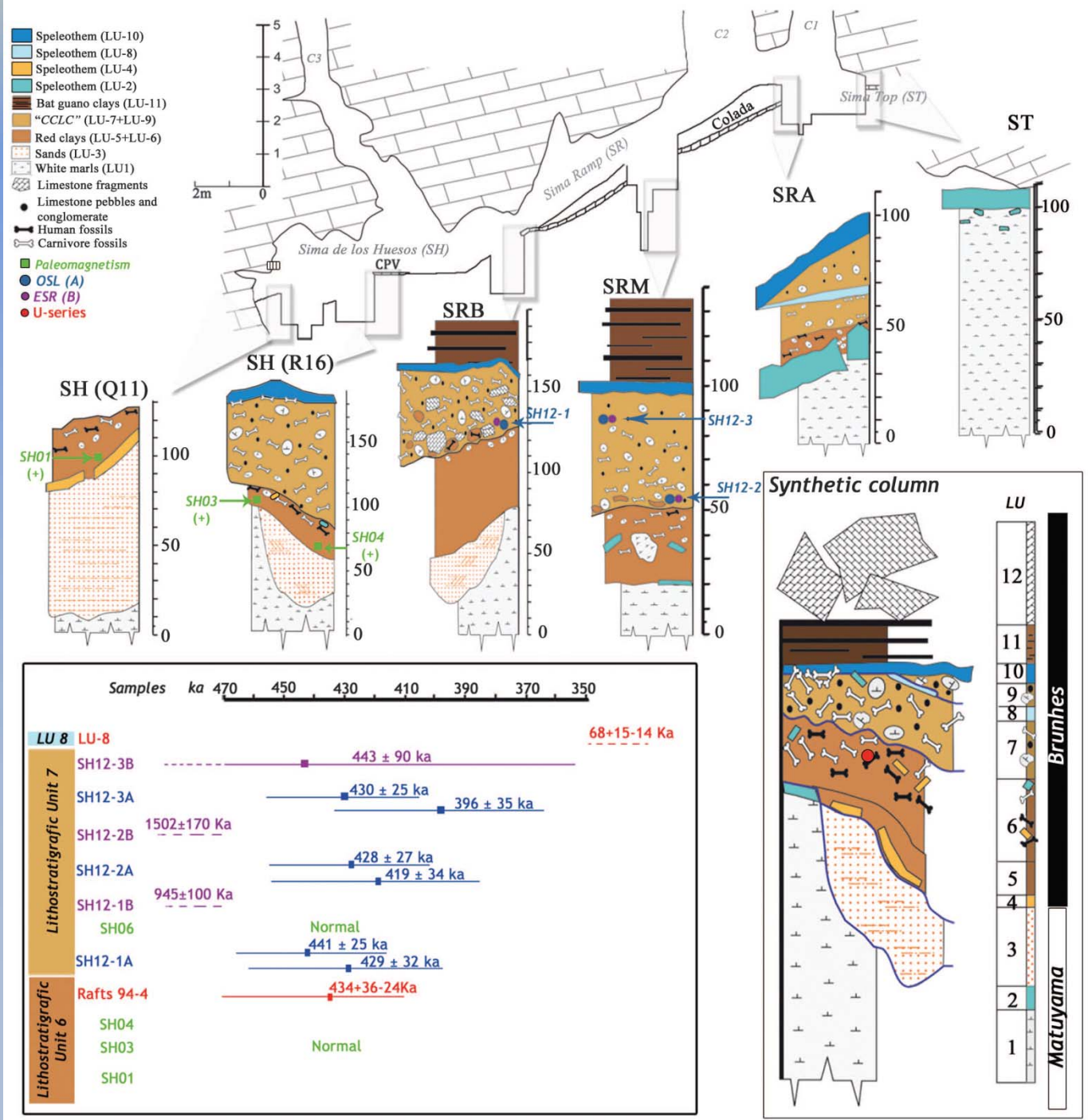




3 cm



Sima de los Huesos, Atapuerca



Arsuaga et al., Science, 2014

Measurement of Palaeodose DE

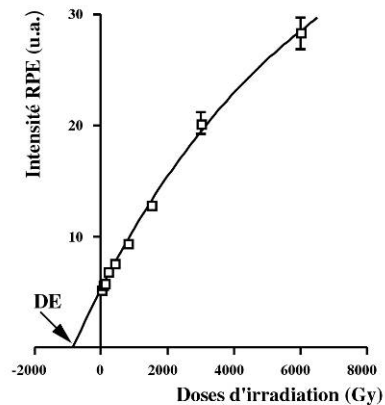
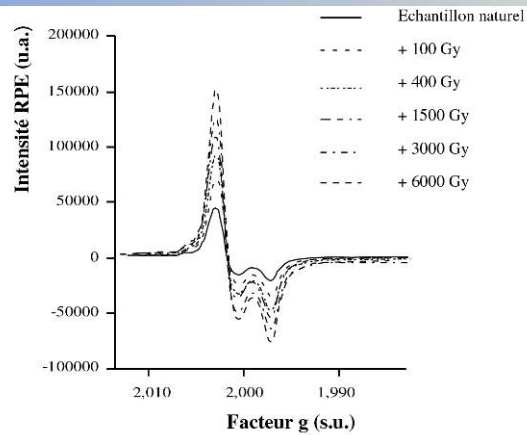


Figure 4 : Croissance du signal à l'irradiation et détermination de la DE par la méthode de l'addition en utilisant une extrapolation exponentielle.

ESR method

$$\text{AGE} = \text{DE} / d_a$$

Measurement of the annual dose, d_a

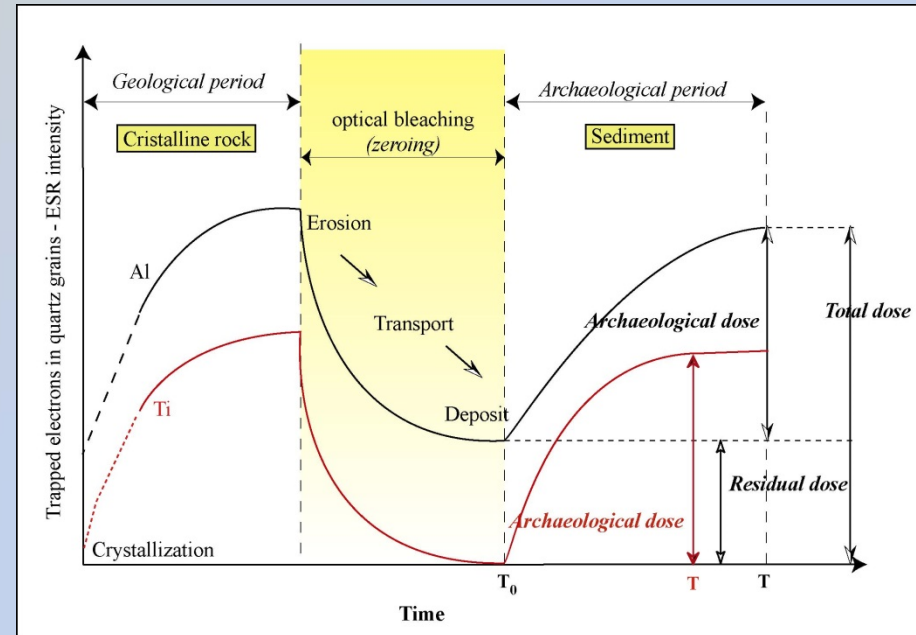
U, Th + daughters, K



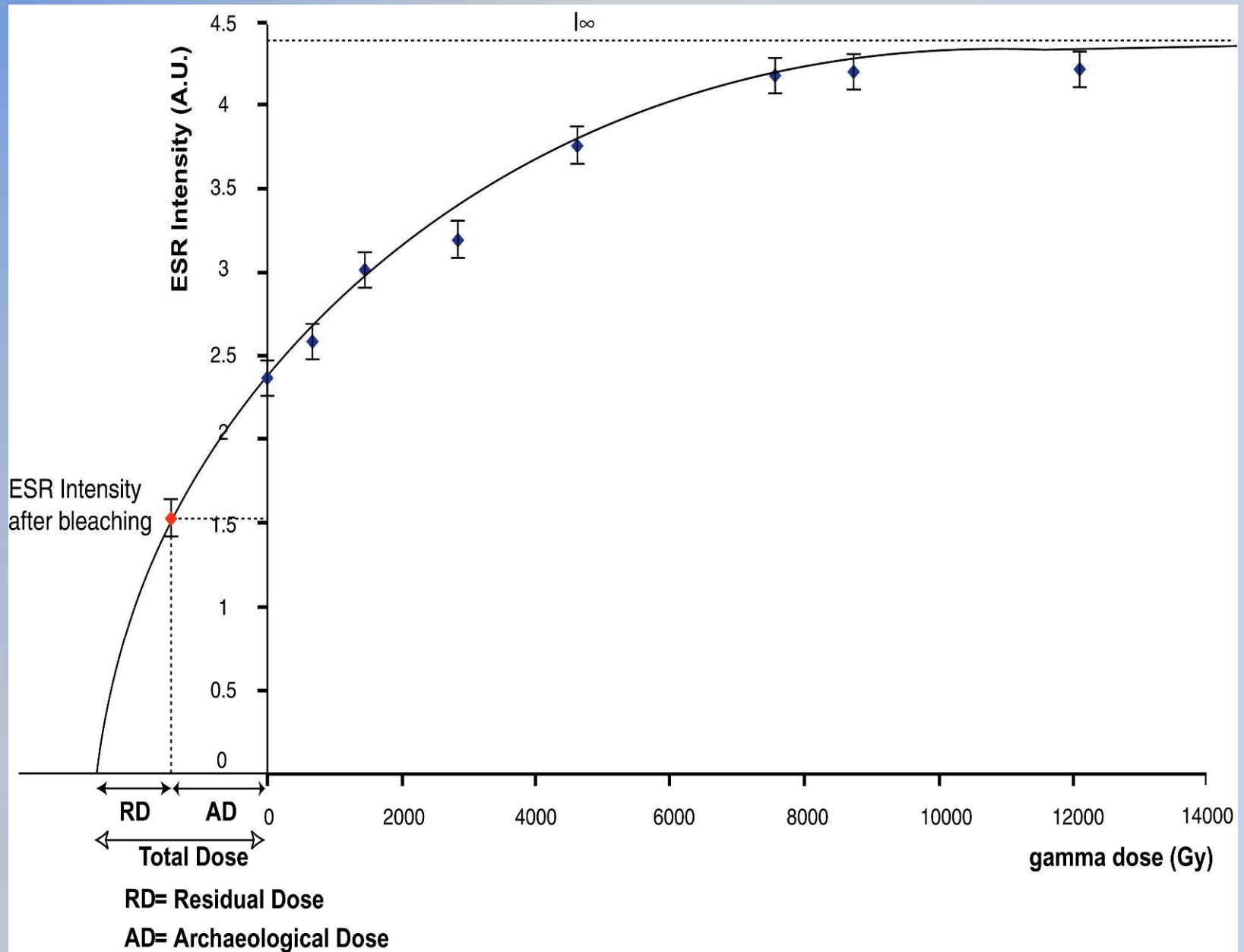
ESR Dating - Quartz



Frequent material



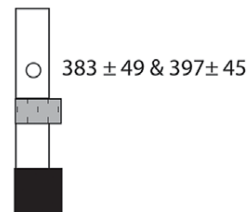
... but no complete bleaching



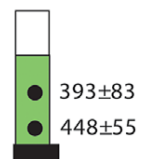
ENGLAND

Post MIS12 sites

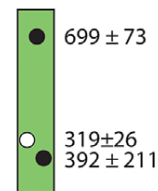
Beeches Pit



East Farm
Barnham



Purfleet

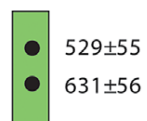


Pre MIS12 sites

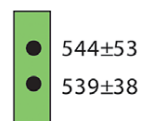
Brooksby



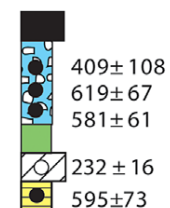
Maidcross Hill



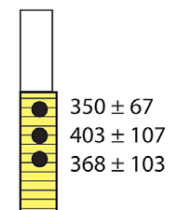
Warren Hill



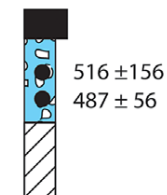
Pakefield



Valdoe



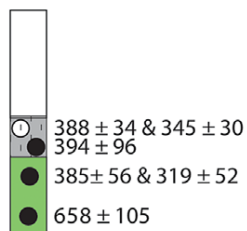
West Runton



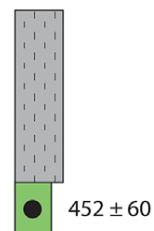
FRANCE

Post MIS12 sites

Saint-Pierre-
lès-Elbeuf

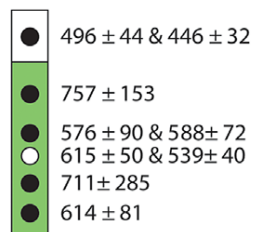


La-Celle-
sur-Seine

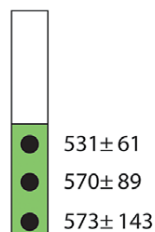


Pre MIS12 sites

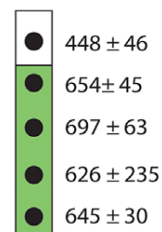
Abbeville
Carrière Carpentier



Amiens
Rue du Manège



La Noira



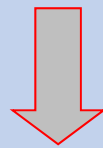
- ESR/U-series age on teeth
- ESR age on sediment
- Fluvial sediments
- Shallow marine sediments
- Fluvio-glacial sediments
- Cover deposits
- Tufa
- MIS12 Till
- Cromer Forest Bed (CfB)

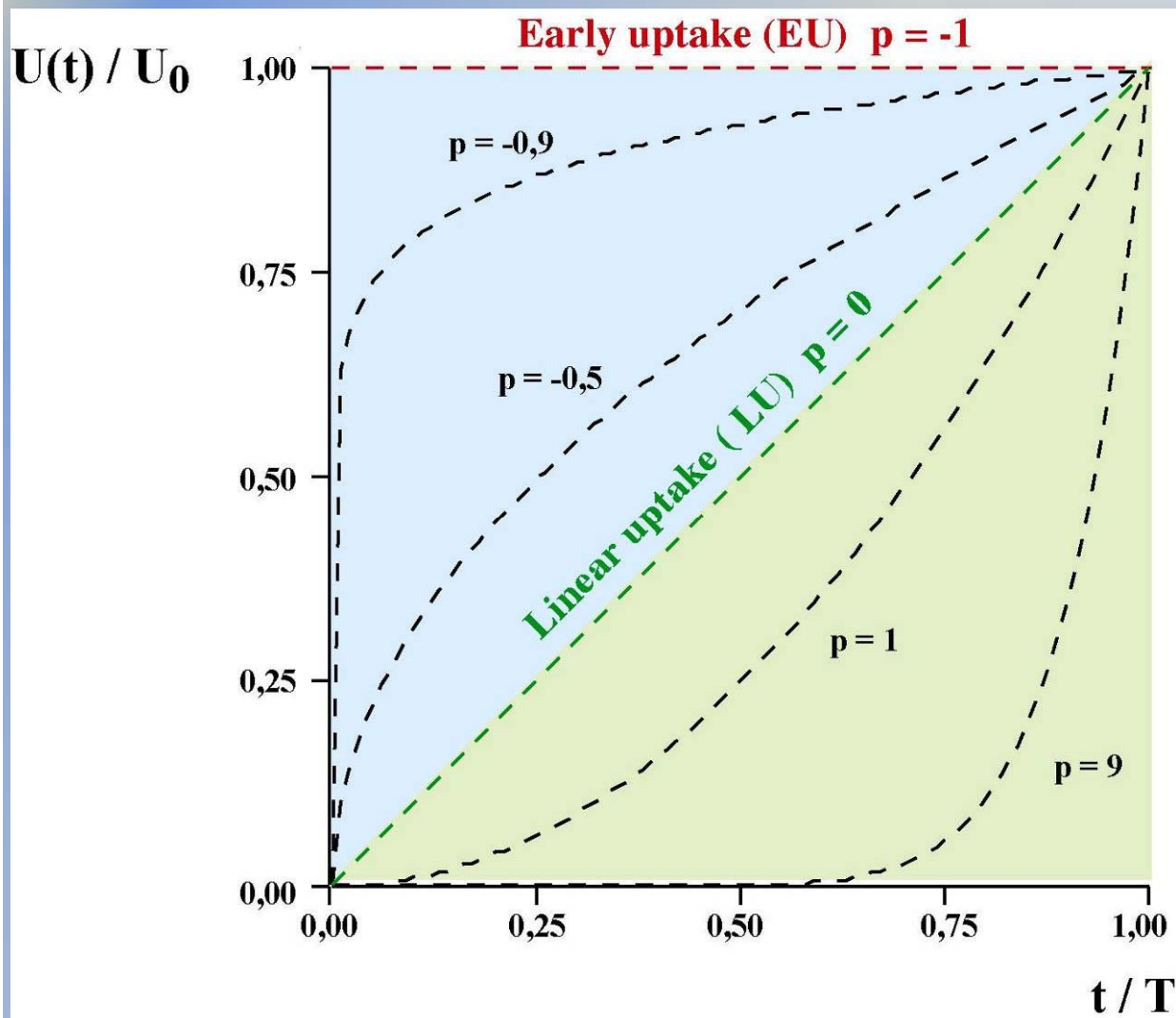
Combined ESR/U-Th Dating - Dental enamel

Direct Dating of human bearing occupation layers



but post-mortem uranium uptake
should be taken into account in the
annual dose calculation





$$U(t) = U_0(t/T)^{p+1}$$

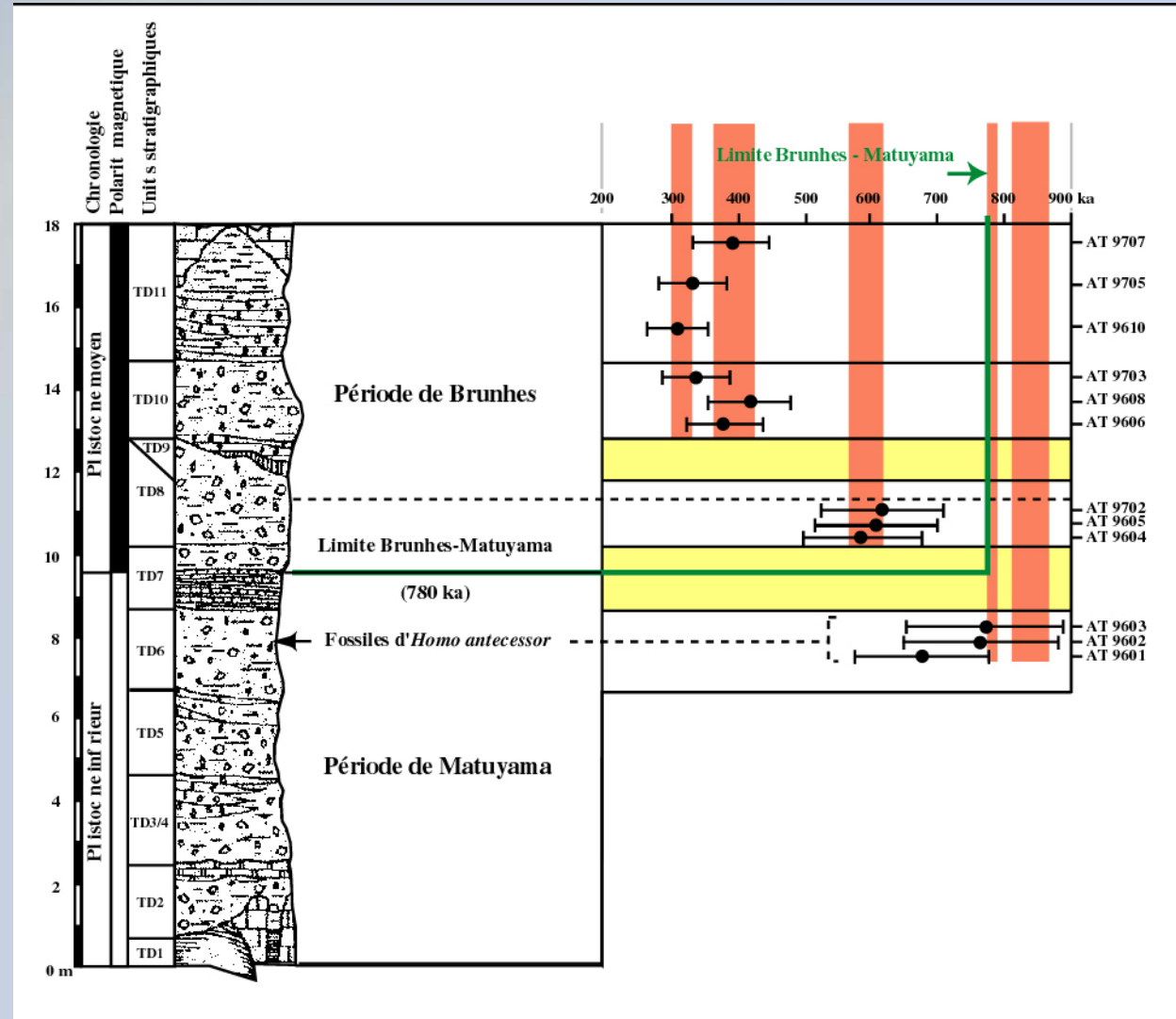
ESR Ages < U-Th Ages
 => U leaching, no age calculation

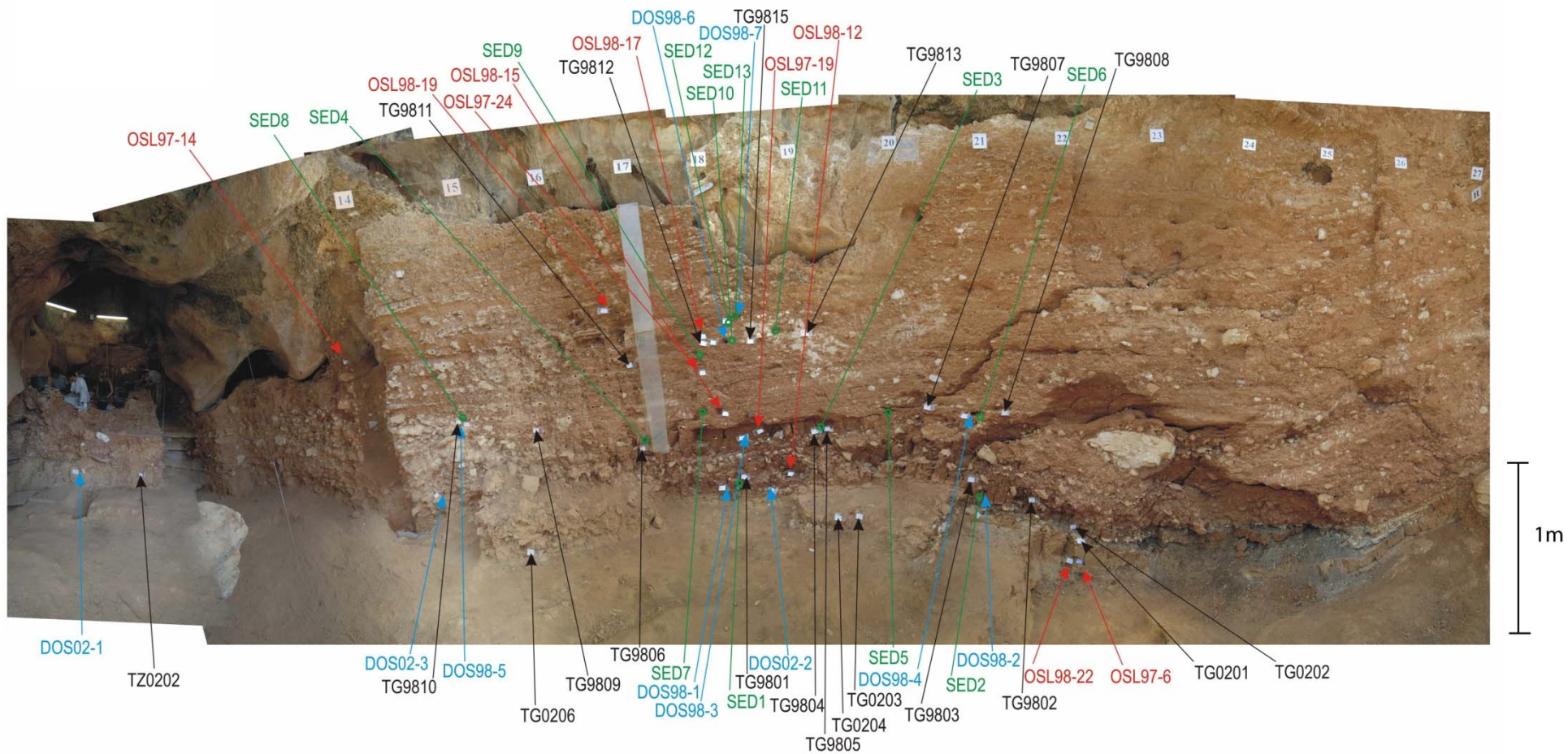
$-1 < p < 0$ area where ages are «acceptables»

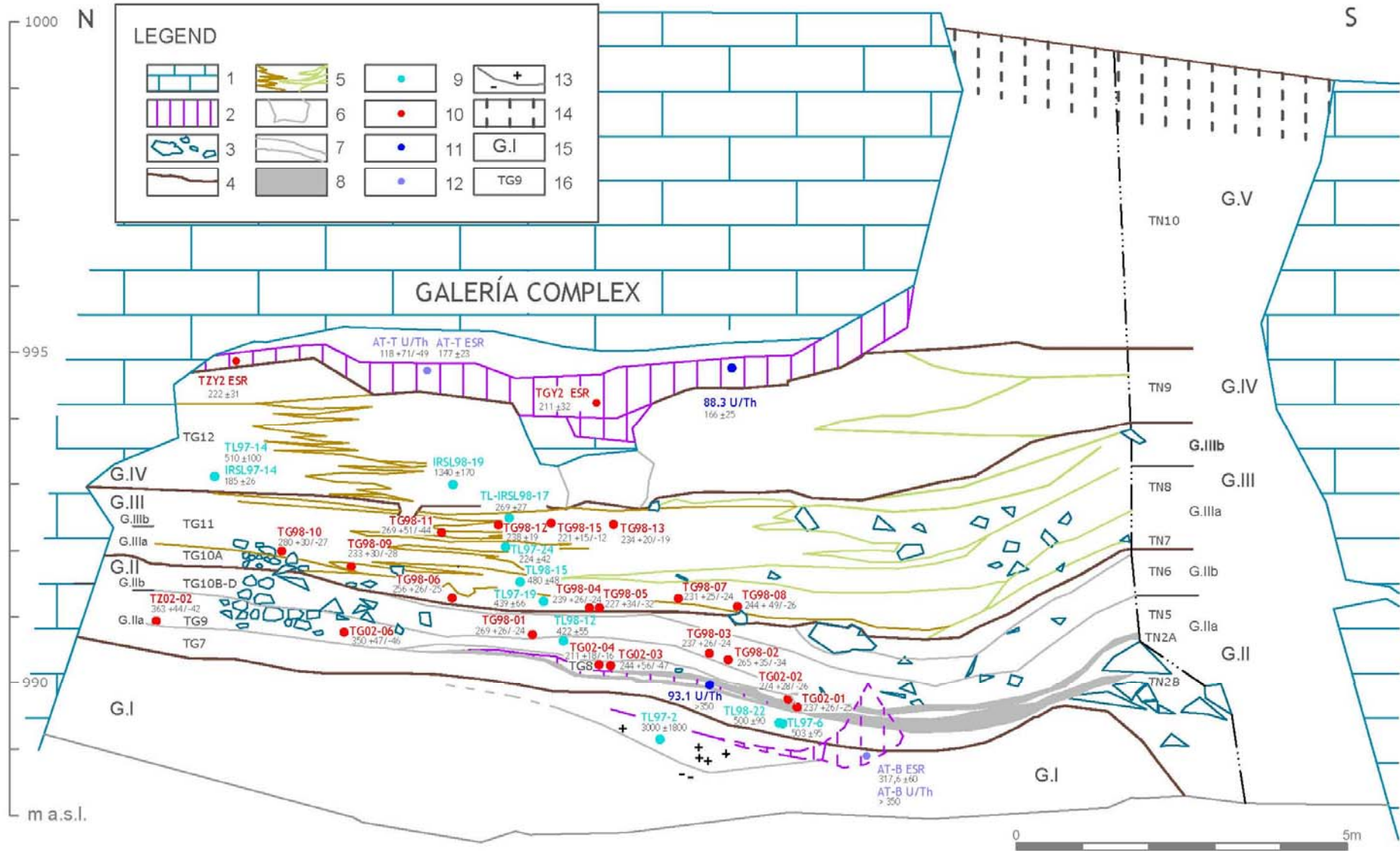
$p > 0$ recent uranium uptake

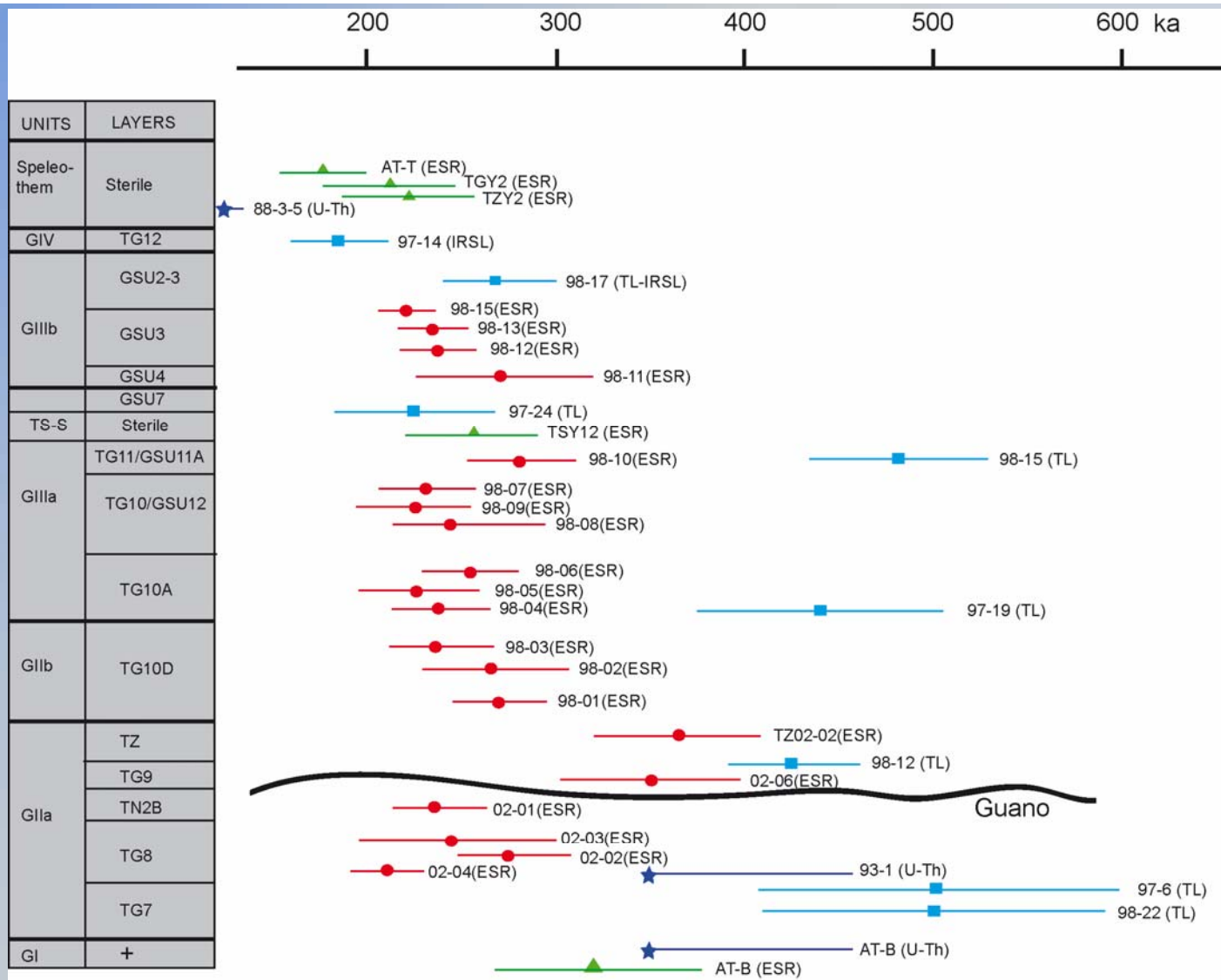
Grün et al., Nuclear Tracks, 1988

Application - Atapuerca Gran Dolina

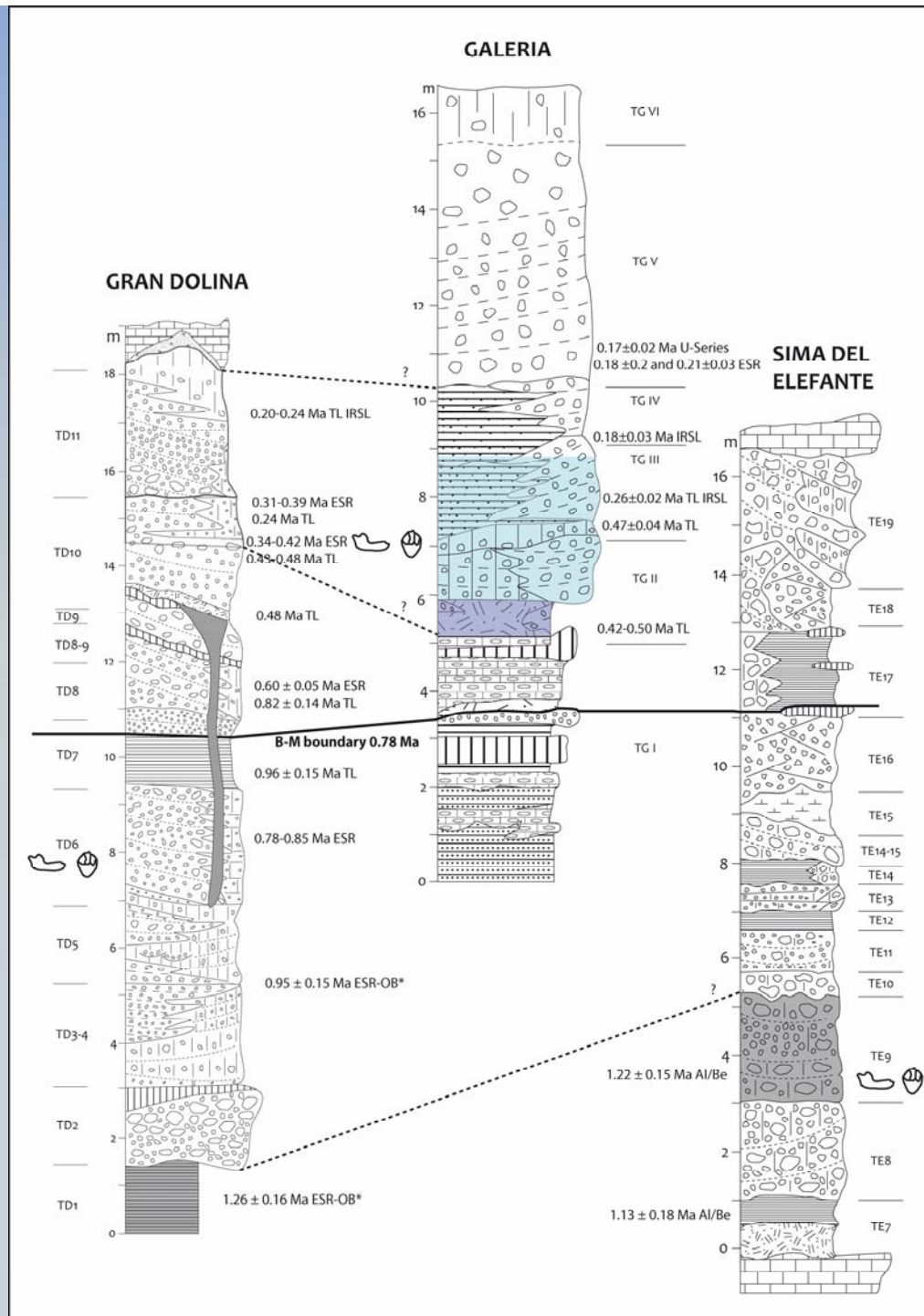








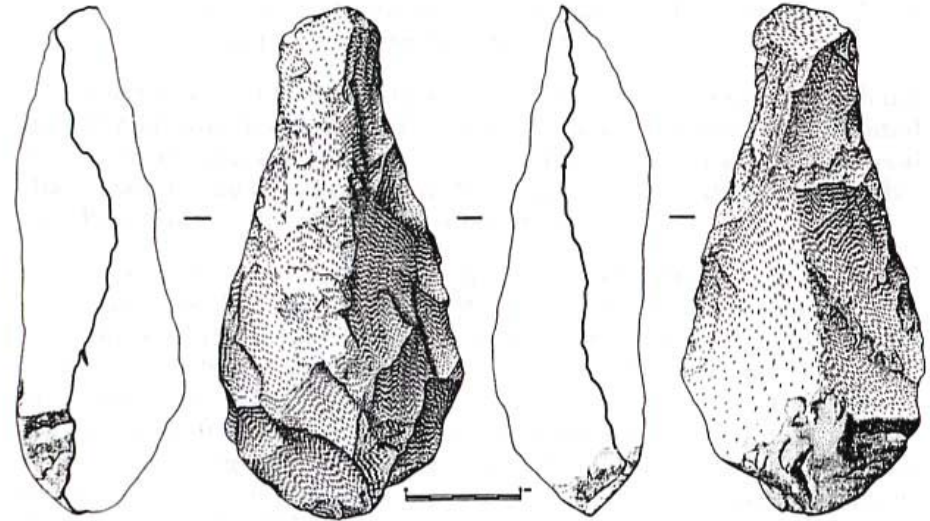
- combined ESR-U/Th on teeth (this work)
- IRSL and TL ages on sediments (Berger et al., 2008)
- ▲ ESR ages on calcite (Falguères, 1986; Grün and Aguirre, 1987)
- ★ U-series ages on calcite (Bischoff, unpublished; Grün and Aguirre, 1987)



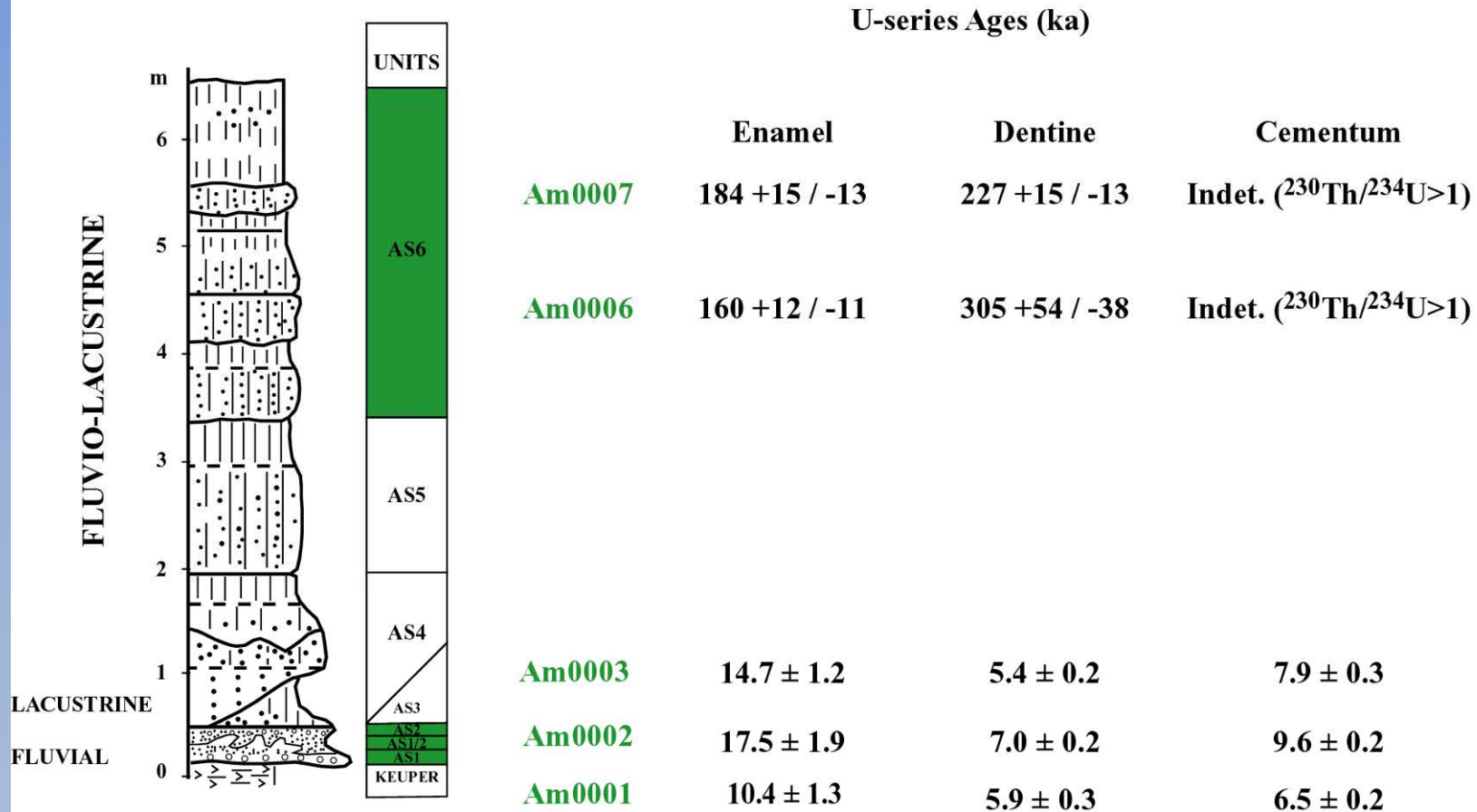


AMBRONA, SPAIN

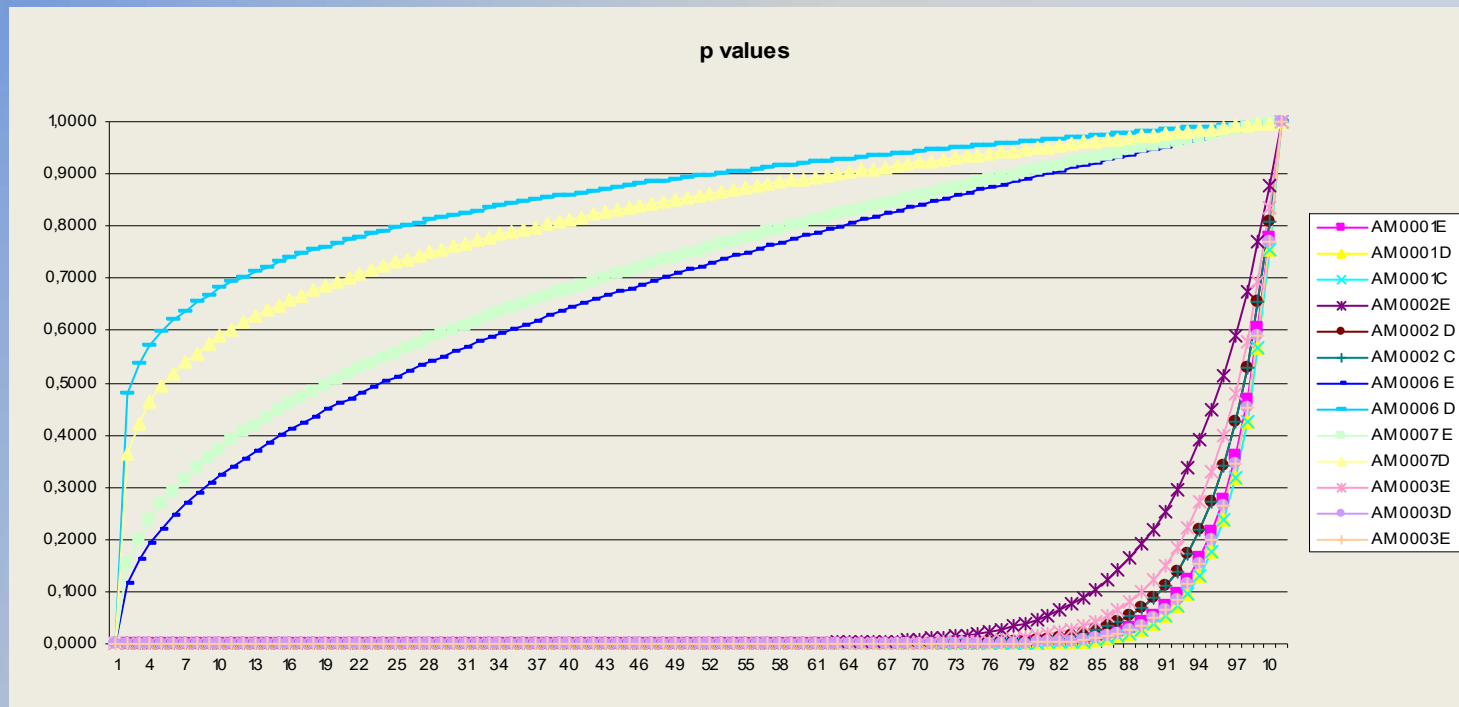
Elephas antiquus
89% of the remains
discovered in 1995
Cervidae
Bovidae
Equidae



AMBRONA



Lithostratigraphic units of the Lower complex of Ambrona (after Perez-Gonzalez et al., 1999)

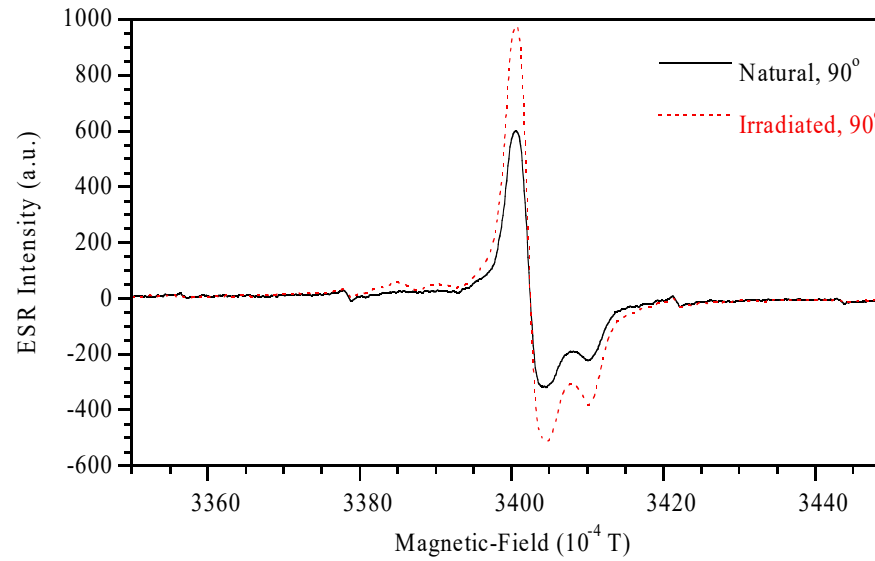
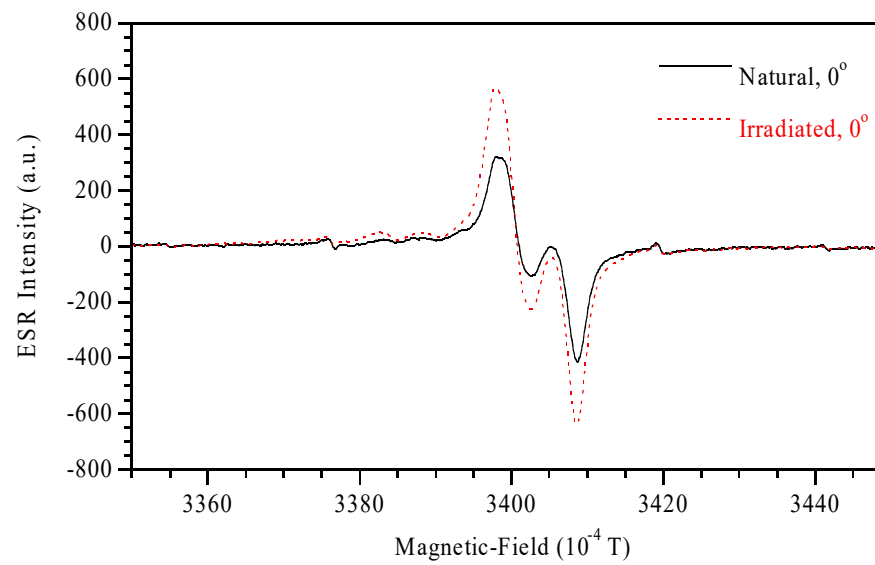
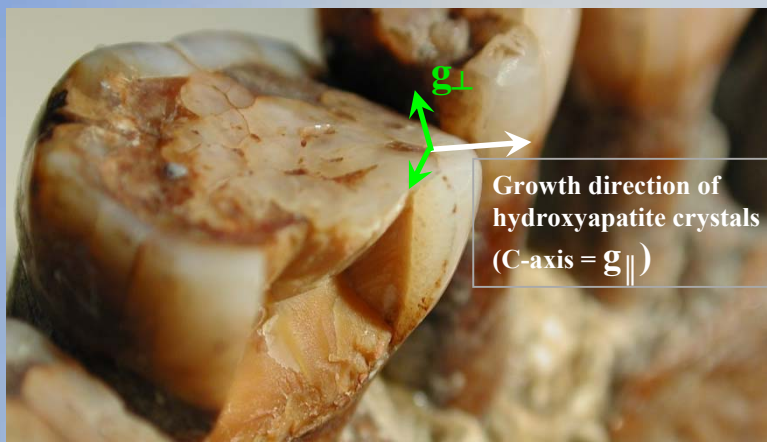


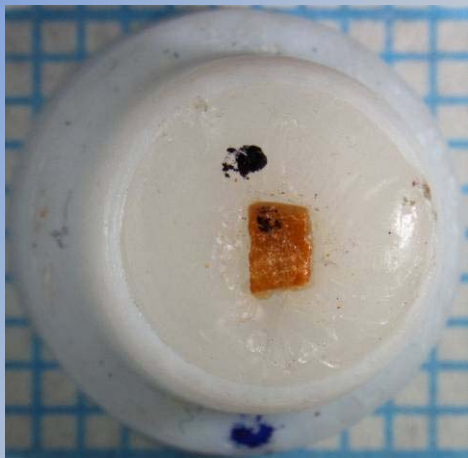
| | p enamel | p dentine | p cementum | Age (ka) |
|---------------|-----------------|------------------|-------------------|----------------------|
| Am0007 | -0.59 | -0.78 | -1* | 366 +55 / -51 |
| Am0006 | -0.53 | -0.84 | -1* | 314 +48 / -45 |
| Am0003 | 17 | 25 | 25 | 316 ± 26 |
| Am0002 | 12 | 20 | 20 | 284 ± 17 |
| Am0001 | 24 | 27 | 27 | 286 ± 29 |

**ESR-U-Th dating of human remains
(Grün, 2006)**



Direct dating Tabun mandible important in the frame of burial in order to check with TL dates performed on quartz extracted from the layers..





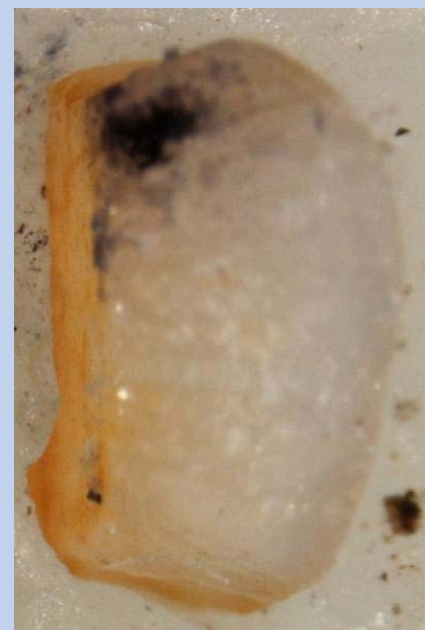
BHS

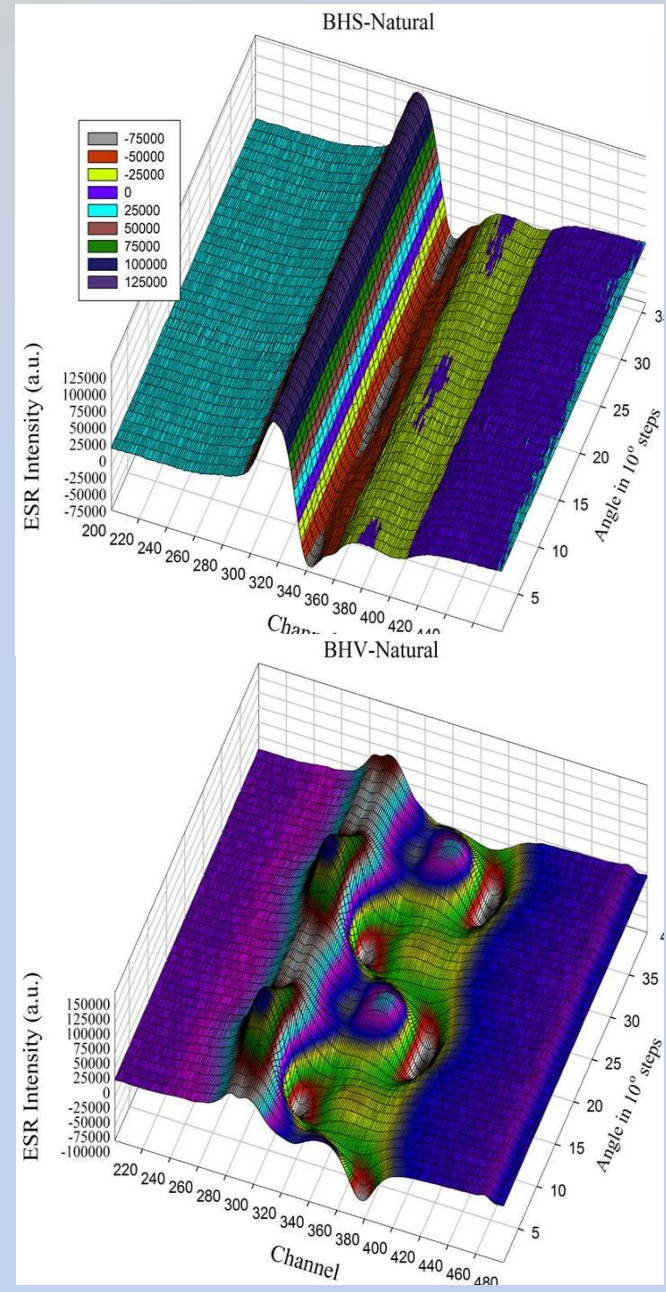
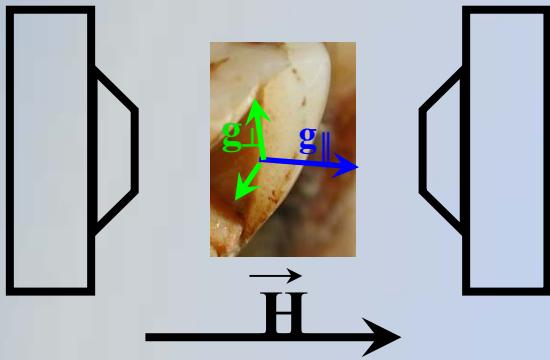
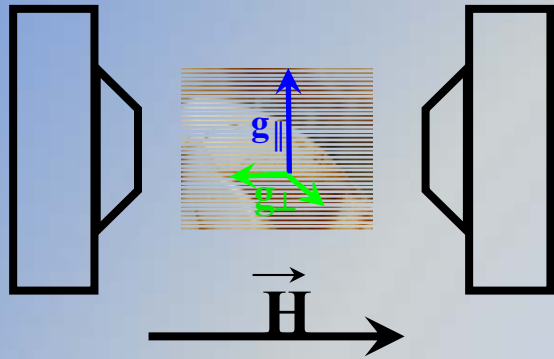


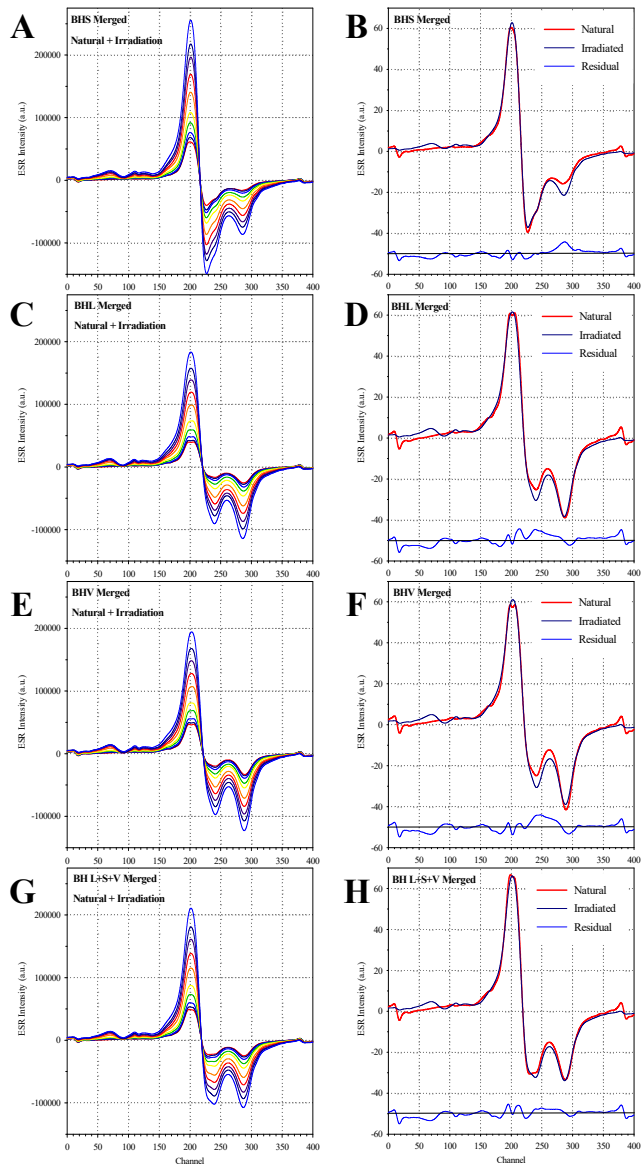
BHL



BHV







- When the spectra are merged, it behaves like a powder (mainly CO₂-radicals):

- There are two different CO₂-radicals, one orientated (**AICORs**), one non-orientated (**NOCORs**) giving rise of a powder spectrum at all angles).

- The thermal stability of the non-orientated CO₂-radical is significantly less than the orientated.

